A comparison of the square wave response of three microscopes commonly used in photointerpretation

A COMPARISON OF THE SQUARE WAVE RESPONSE OF THREE MICROSCOPES COMMONLY USED IN PHOTOINTERPRETATION

by

Ross Brian Hooker III

A Thesis Submitted to the Faculty of the

COMMITTEE ON OPTICAL SCIENCES

In Partial Fulfillment of the Requirements
For the Degree of

MASTER OF SCIENCE

In the Graduate College

THE UNIVERSITY OF ARIZONA

1970

STATEMENT BY AUTHOR

This thesis has been submitted in partial fulfillment of requirements for an advanced degree at The University of Arizona and is deposited in the University Library to be made available to borrowers under rules of the Library.

Brief quotations from this thesis are allowable without special permission, provided that accurate acknowledgment of source is made. Requests for permission for extended quotation from or reproduction of this manuscript in whole or in part may be granted by the head of the major department or the Dean of the Graduate College when in his judgment the proposed use of the material is in the interests of scholarship. In all other instances, however, permission must be obtained from the author.

SIGNED: Ross Brian Hooker III

APPROVAL BY THESIS DIRECTOR

This thesis has been approved on the date shown below:

Jack D. Gaskill

JACK D. GASKILL
Assistant Professor of Optical Sciences

17 Jan. 1970

Date

ACKNOWLEDGMENTS

The author wishes to extend his appreciation to his thesis director, Dr. Jack D. Gaskill, for his continued assistance during this study and to Dr. Roland V. Shack for his illuminating discussions.

Much of the equipment for this study was loaned to the author by the following organizations whose interest and assistance is gratefully acknowledged: The Reconnaissance Engineering Section of Rome Air Development Center, Griffiss Air Force Base, New York, provided the Bausch & Lomb 240 stereomicroscope, the Olympus SZ III stereomicroscope, and much of the test equipment; Wild Heerbrugg Instruments, Inc. provided a Wild M-5 stereomicroscope; Bausch & Lomb, Inc. provided a prototype 2X auxiliary objective for their microscope, and Richards Corporation provided a sample of the diffuser used on their light tables.

TABLE OF CONTENTS

TABLE OF CONTENTS--Continued

LIST OF ILLUSTRATIONS

LIST OF ILLUSTRATIONS--Continued

LIST OF ILLUSTRATIONS--Continued

LIST OF TABLES

ABSTRACT

The optical performance of three stereomicroscopes commonly used for photointerpretation is described in terms of magnification, field of view, and Square Wave Response (SqWR). For a given field size, the Square Wave Response can be used to compare the amount of information in the image of each microscope. The Square Wave Response was determined by scanning a square wave test target at four field positions for each of four field sizes (corresponding to magnifications of 6, 12, 25 and 50X). The measured Square Wave Response was used to evaluate the relative ability of each microscope to perform two typical photointerpretation tasks: (1) scanning or searching for a target, and (2) detailed viewing of a target. For these tasks the Wild M-5 stereomicroscope was found to be somewhat superior to the Bausch and Lomb 240 stereomicroscope, and both were found to be better than the Olympus SZ III stereomicroscope. The Square Wave Response curves are included and can be used to compare the stereomicroscopes for their photointerpretation tasks.

CHAPTER I

INTRODUCTION

Many types of microscopes are used by photointerpreters as an aid in viewing aerial reconnaissance imagery. Often it is necessary to compare these microscopes and evaluate their usefulness in a particular photointerpretation situation. In some cases the microscope characteristics of interest can not be directly measured, and related quantities must be measured and properly interpreted in order to obtain the desired information. For example, operator fatigue caused by looking through a microscope is difficult to measure directly. However, quantities such as the film-to-eyepoint distance, eyepiece inclination and eye relief can be measured and may help indicate the expected operator fatigue. In a similar way, direct measurement of the optical properties of a microscope can be used to express such characteristics as the quality of the image and the amount of information transmitted by the microscope.

The optical system of a microscope used in photointerpretation is usually described in terms of its magnification, field of view and resolution. Each of these is measurable and influences the photointerpreter's impression of image quality and information transfer. The resolution gives an idea of the finest detail (or maximum information density) that can be imaged through the microscope. When the field of

view is also stated, we have an indication of the maximum amount of information that may be contained in the microscope image. The magnification of the microscope determines how well the eye can receive the image. That is, the finest detail resolved by the microscope must be magnified sufficiently to be resolved by the eye.

Unfortunately, this description of a microscope is unnecessarily restrictive, since it refers only to the ability of the microscope to resolve very fine detail. It does not directly indicate how well the microscope can image a general object distribution. The description takes on substantially more meaning if we characterize the microscope by the modulation transfer function (MTF) or sine wave response (SWR), rather than resolving power. In going to the more complete description, the convenience of characterizing the microscope by a single number is lost. However, the gain in information is well worth the additional complexity.

In this paper the optical properties of three microscopes commonly used in photointerpretation are compared. The comparison is based on magnification, field of view and the square wave response (SqWR), a relative of the sine wave response. In Chapter 2 the meaning of and relationship between SWR and SqWR is discussed, and the technique used to measure SqWR is described. A description of the microscopes is given in Chapter 3. Chapter 4 is concerned with the equipment and techniques used to measure the SqWR, and in Chapter 5 the resulting SqWR curves are presented. In Chapter 6 the curves are interpreted, and the microscopes are compared.

CHAPTER 2

SINE WAVE AND SQUARE WAVE RESPONSE FUNCTIONS

Sine Wave Response

Fourier analysis permits the expression of an arbitrary irradiance distribution as a linear combination of sinusoidal components of appropriate phase and amplitude. If the irradiance distribution of an incoherently illuminated object is expressed in this fashion, then each sinusoidal component is transmitted through a linear optical system unaltered in frequency, although the phase of each component may be shifted and its amplitude reduced.

The optical transfer function (OTF) of an incoherent optical system relates the spatial frequency spectrum, $\tilde{O}(s)$, of the object irradiance distribution to the spatial frequency spectrum, $\tilde{I}(s)$, of the image irradiance distribution, and is given by (Shack 1956, Goodman 1968)

$$\text{OTF} = \frac{\tilde{I}(s)}{\tilde{O}(s)} \quad .$$

In general the OTF is complex since it describes how the optical system alters both the amplitude and phase of the sinusoidal components. The modulus of the OTF is just the sine wave response of the optical system and thus

$$\text{SWR} = |\text{OTF}| = \left|\frac{\tilde{I}(s)}{\tilde{O}(s)}\right| = \frac{|\tilde{I}(s)|}{|\tilde{O}(s)|} \quad . \qquad (1)$$

The SWR contains no information about the phase of the sinusoidal components.

The value of $|\tilde{I}(s)|$ or $|\tilde{O}(s)|$ at a particular spatial frequency is equal to the modulation of the sinusoidal irradiance component of that frequency. The modulation, M, is defined in the usual way as

$$M = \frac{I_{max} - I_{min}}{I_{max} + I_{min}}, \qquad (2)$$

Where I_{max} and I_{min} are the maximum and minimum values of the irradiance of the sinusoidal component. Thus, for a particular sinusoidal component the SWR is numerically equal to the fractional reduction of modulation when that component is transferred from the object plane to the image plane.

One method for determining the SWR of an optical system is to measure the reduction of modulation for various sinusoidal irradiance components as they pass through the system. This can be done by placing sinusoidal test targets of known modulation in the object plane of the optical system and then scanning the sinusoidal image distributions with a pinhole to find the maximum and minimum values of irradiance (Department of Defense 1962, p. 26.12). The modulation of the image is then calculated from Equation (2), and the reduction of modulation is calculated from Equation (1).

Square Wave Response

Because it is quite difficult to fabricate high-quality, high-resolution sinusoidal test targets (Department of Defense 1962, p. 26.17),

square wave test targets, which are much easier to make, are often used. The modulation of the square wave irradiance distribution, like the modulation of a sine wave distribution, is defined by Equation (2). If a square wave irradiance distribution of frequency s and modulation $|\tilde{O}_{sq}(s)|$ is placed in the object plane of an optical system, and if the modulation of the image irradiance distribution is denoted by $|\tilde{I}_{sq}(s)|$, then the square wave response of the optical system is defined to be

$$\text{SqWR} = \frac{|\tilde{I}_{sq}(s)|}{|\tilde{O}_{sq}(s)|} \quad . \tag{3}$$

Although there is a striking similarity between Equations (1) and (3) there exist fundamental differences in the meaning that can be given to each expression. Equation (1) describes the reduction of modulation of the sinusoidal irradiance components that are transferred from an object plane to an image plane by an optical system. Equation (3) describes a similar reduction of modulation when the object is expressed as a combination of square wave irradiance components. However, square waves, unlike sine waves, are not invariant in passing through an optical system; the image of a square wave object is not a square wave, even though it normally has the same fundamental frequency as the object. The consequence of the noninvariance of square waves is that Equation (3) cannot be used to predict the image distribution for an arbitrary object distribution that is expressed as a combination of square waves. If such a predicition is required, we must use the sine wave relationship of Equation (1).

Since the SqWR is easier to measure than the SWR but cannot be used to predict image distributions from object distributions, we may want to convert a measured SqWR to the SWR. Coltman (1954) has shown that the SWR, T(s) here, at spatial frequency s can be expressed in terms of the SqWR, $T_{sq}(s)$ here, by

$$T(s) = \frac{\pi}{4}\left[T_{sq}(s) + \frac{T_{sq}(3s)}{3} - \frac{T_{sq}(5s)}{5} + \frac{T_{sq}(7s)}{7} \ \ldots\ \right] , \tag{4}$$

where the SWR and SqWR are now denoted by T(s) and $T_{sq}(s)$, respectively. Curves of both the SWR and the SqWR are plotted in Figure 1 for a diffraction limited circular aperture.

In the diffraction limited case of Figure 1, the SqWR is at least as great as the SWR for all spatial frequencies; but when aberrations are present this is not necessarily true. Using Equation (4) we can calculate the SWR in different spatial frequency regions and compare the SqWR with the SWR (Scott, Scott and Shack 1963).

Region	SWR
A: $\left(S > \frac{S_{max}}{3}\right)$	$\frac{\pi}{4} T_{sq}(s)$
B: $\left(\frac{S_{max}}{5} < S < \frac{S_{max}}{3}\right)$	$\frac{\pi}{4} T_{sq}(s) + \frac{\pi}{12} T_{sq}(3s)$
C: $\left(\frac{S_{max}}{7} < S < \frac{S_{max}}{5}\right)$	$\frac{\pi}{4} T_{sq}(s) + \frac{\pi}{12} T_{sq}(3s) - \frac{\pi}{20} T_{sq}(5s)$

In region A the SqWR is always greater than the SWR, and in region B the SqWR is greater if $T_{sq}(3s) < 0.82\ T_{sq}(s)$. If the SqWR is greater

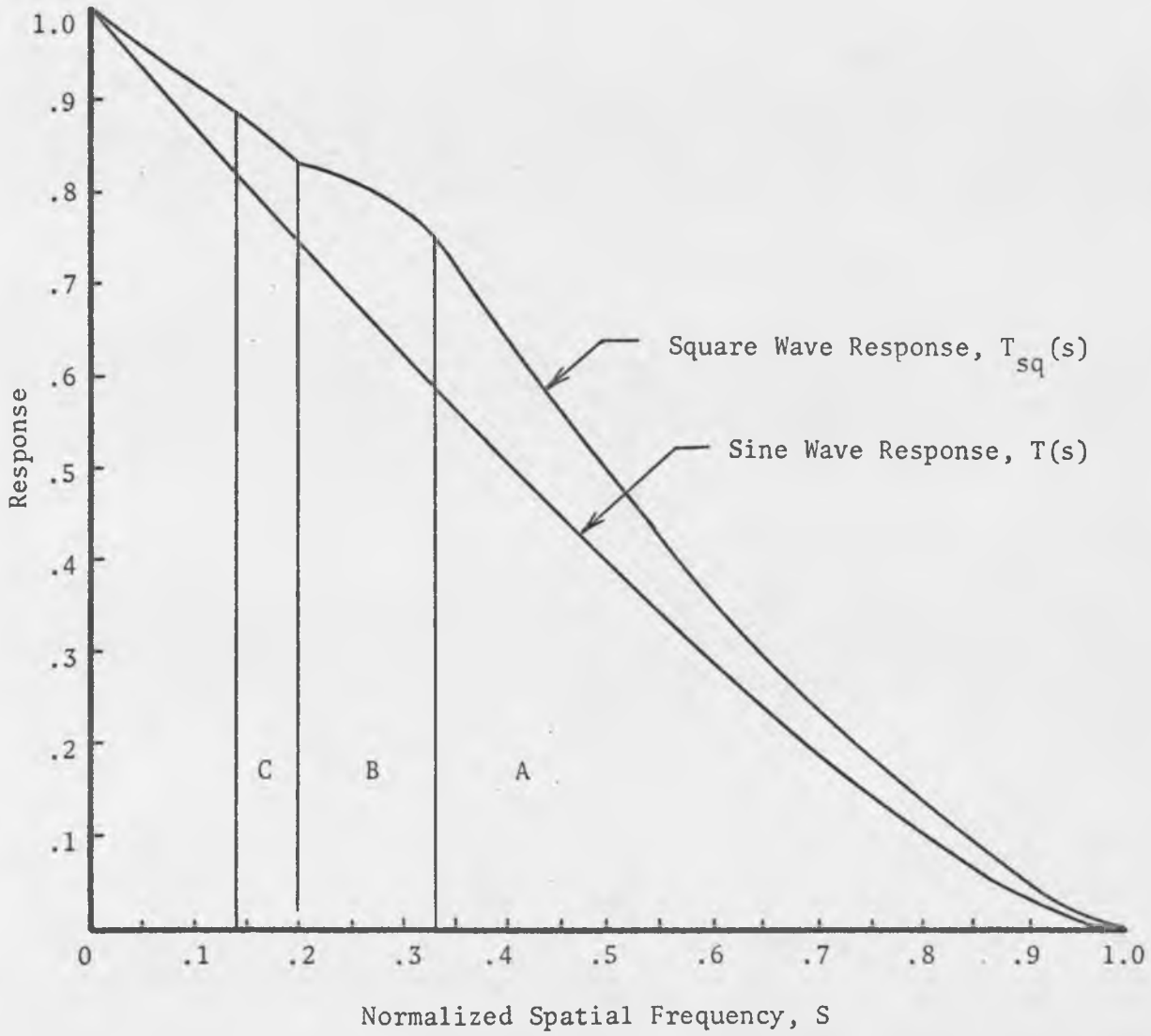

Fig. 1. Sine Wave Response and Square Wave Response for a Diffraction Limited, Circular Aperture

than the SWR in region B, it must also be greater in region C. Therefore, for an aberrated optical system the SqWR is greater than the SWR over 85 percent of the spatial frequency range (regions A, B and C) for the condition $T_{sq}(3s) < 0.82\ T_{sq}(s)$. This is the case for optical systems with circular apertures when the aberrations are not too severe. However, even if the above condition is not met, the SqWR will not be significantly less than the SWR provided the values of $T_{sq}(3s)$ and $T_{sq}(5s)$ are sufficiently small (about 0.1 or less). In all but a few cases, the SqWR of the microscopes in this study satisfies one of these conditions, insuring that the SqWR is greater than the SWR.

A consequence of this relationship between the SqWR and SWR is that many optical systems, including the microscopes in this study, can be compared equally well using either SqWR or SWR. That is, if system A is "better" than system B by comparison of their SqWR, then it will also be "better" by comparison of their SWR. In this case, "better" means having a higher response over a larger frequency range.

Thus, there are two ways in which we can ascribe meaning to SqWR curves. First, we can convert SqWR to SWR and, thereby, be able to predict image distributions from object distributions. Secondly, we can use SqWR as a basis of comparing optical systems. In the remainder of this paper we shall be concerned with using the SqWR as a comparison tool.

The Measured Square Wave Response

The SqWR of the microscopes was measured for the same conditions under which they are used. In this way, a direct comparison of microscope

performance can be made without having to transform test conditions into operational conditions. Normally the microscopes are used on a light table where aerial imagery is backlighted with diffuse illumination (for example, Figure 2 in Chapter 3). A fluorescent source illuminates a plastic diffuser which is positioned 1/4 inch to 2 inches (depending on the light table) behind the film being viewed. Three characteristics of this diffuse illumination affect the SqWR measurements: (1) the broad spectral band (white) of the fluorescent source, (2) the position of the object plane relative to the diffuser, and (3) the size of the illuminated diffuser. Each of these characteristics and its effect on the SqWR will be considered in Chapter 4.

As discussed earlier, we wish to compare information transfer and image quality indirectly by performing a direct comparison of the magnification, field of view, and SqWR of the microscopes. If the magnification is sufficiently large, then the information transfer is some function of both SqWR and field of view (but not magnification). Not knowing what this function is, we can compare information transfer by comparing the SqWR at a constant field of view. Of course, we could also measure the field of view at a constant SqWR, but this is a much more difficult task. Therefore, the basis of comparing the microscopes will be the SqWR with the microscopes adjusted to the same field of view.

CHAPTER 3

THE MICROSCOPES

Three microscopes have emerged as the predominant ones for photointerpretation--the Bausch and Lomb 240, the Olympus SZ III and the Wild M-5. They are characterized by relatively low magnifications (less than 100X) and low numerical apertures (less than 0.18) and all have two optical channels whose optical axes intersect at the object plane. Generically they should be called stereomicroscopes since they provide a stereo presentation when viewing a three dimensional object. However, when viewing aerial imagery the display is two-dimensional and the stereomicroscope is functionally a microscope. Hereafter, the term microscope will be used to mean stereomicroscope.

All three microscopes can be converted to stereoscopes (actually microstereoscopes if we need to distinguish them from the common "pocket stereoscope") by attaching rhomboid arms to the bottom of the microscope body or pod. With rhomboids, each optical channel can be set to view a different frame of imagery. If there is coverage overlap between the frames, then a stereo presentation can be seen. This study is concerned only with the microscopic, not the stereoscopic, mode of operation.

Figures 2, 3 and 4 are photographs of the microscopes, shown mounted on a typical photointerpretation light table.

Fig. 2. The Bausch & Lomb 240 Stereomicroscope

Fig. 3. The Olympus SZ III Stereomicroscope

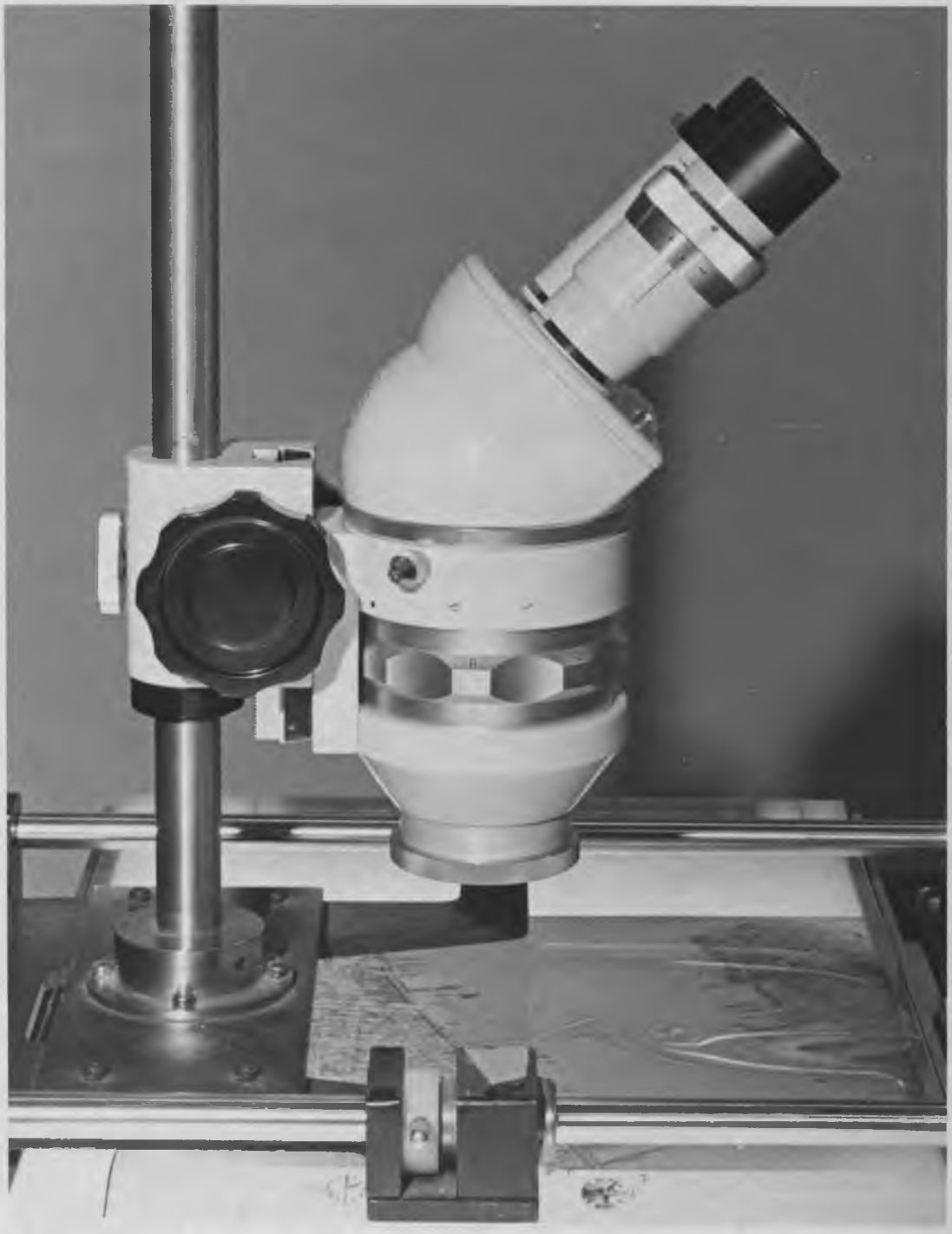

Fig. 4. The Wild M-5 Stereomicroscope

Each microscope consists of eyepieces, auxiliary objectives and a pod containing the primary objectives. In this study 10X eyepieces were used exclusively. The auxiliary objectives screw into the bottom of the microscope pod and are used to halve (0.5X) or double (2X) the magnification provided by the pod and eyepieces. For identification in this study, a microscope at a particular magnification will be assigned a designation of the form B/12/2. The "B" indicates the Bausch and Lomb microscope ("O" for Olympus; "W" for Wild), the "12" indicates the magnification of the pod/eyepiece combination, and "2" indicates the magnification of the auxiliary objective. If no auxiliary objective is used the last designation is "1" since this is equivalent to using a zero power (1X) auxiliary objective. The total magnification of the microscope is the product of the pod/eyepiece magnification and the auxiliary objective magnification (24X in this example).

In Table I, selected characteristics of the three microscopes are listed in order to identify the type of instruments being compared. Table I includes only those eyepieces, pods, and auxiliary objectives used in this study and, as such, does not represent a complete specification. Most of the characteristics were extracted from the manufacturer's literature, and their accuracy was not confirmed or refuted by this study.

The optical configurations of the microscopes are shown in Figure 5. The Bausch and Lomb and Olympus microscopes appear very

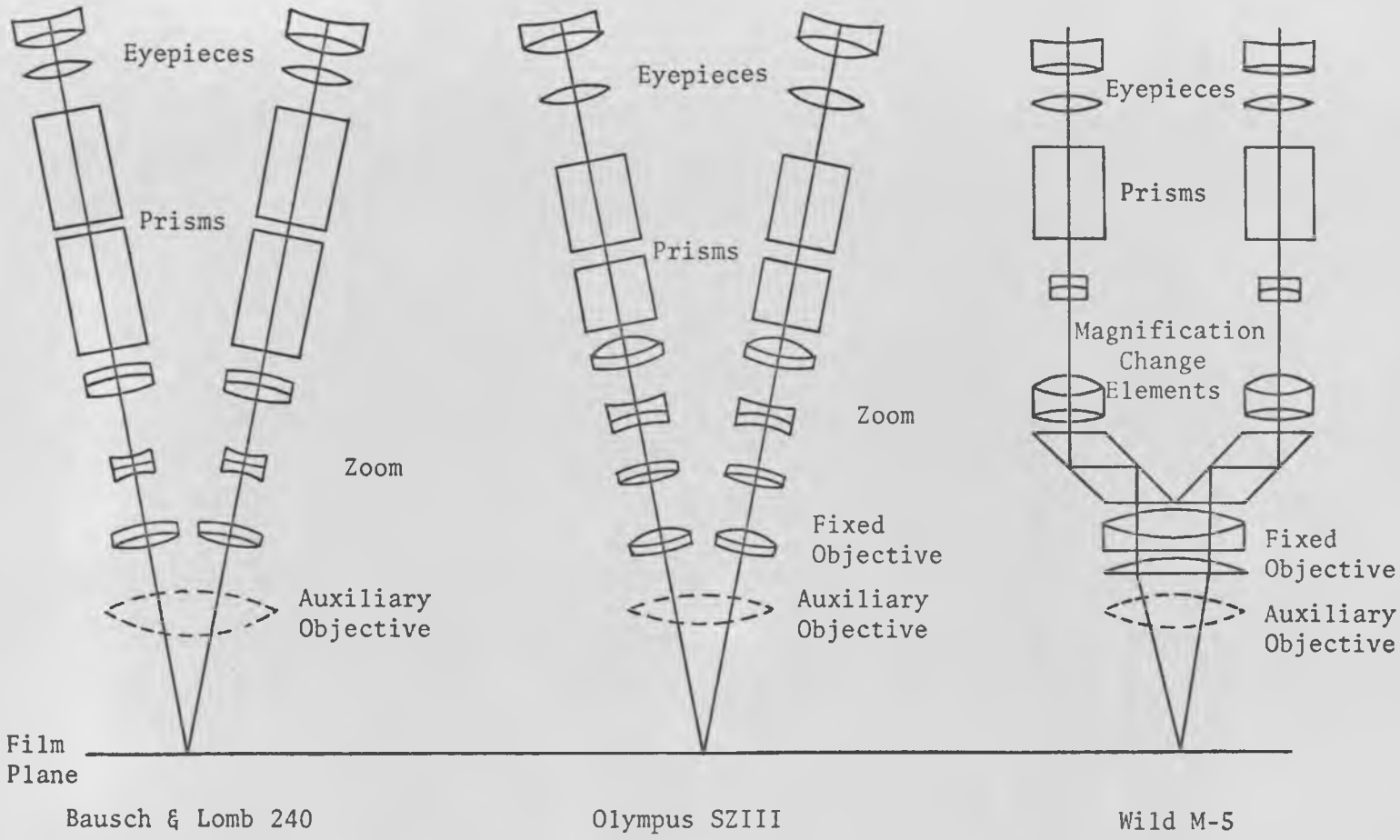

Fig. 5. Optical Configurations of the Microscopes (from the manufacturers' literature)

Table I. Selected Characteristics of the Microscopes

	B&L 240	Olympus SZ III	Wild M-5
Catalog Number			
Microscope Pod	53-70-25	600033*	1000
10X Eyepieces	53-70-96-220	-	1100
0.5X Aux. Obj.	53-70-32	600036*	1107
2X Aux. Obj.	Prototype	600037*	1106
Magnification (with 10X Eyepieces)			
Pod Alone	7-30X	7-40X	6, 12, 25, 50X
With 0.5X Aux. Obj.	3.5-15X	3.5-20X	3, 6, 12, 25X
With 2X Aux. Obj.	14-60X	14-80X	12, 25, 50, 100X
Zoom Range	4:1	5.7:1	None
Resolution (cycles/mm)	240 at 30X	200 at 40X	at least 250 at 50X
Field of View (10X Eyepieces)	196mm ÷ magnification	220 mm ÷ magnification	210 mm ÷ magnification
Interpupillary Separation (mm)	60-72	46-74	55-75
Working Distance (mm)			
Pod Alone	102	97	96
With 0.5X Aux. Obj.	153	166	165
With 2X Aux. Obj.	19	36	33
Filmplane to Eyepoint Distance (mm)			
Pod Alone	309	283	305
With 0.5X Aux. Obj.	394	375	400
With 2X Aux. Obj.	267	238	275

*Richards Corporation Catalog Number

similar; both have completely separate optical channels when no auxiliary objective is used. With an auxiliary objective, both microscopes are cycloptic since each of their optical channels looks nonsymmetrically through the auxiliary objective. The Wild microscope is distinctly different in that it is cycloptic for all magnification ranges--both with and without its auxiliary objectives. Since cycloptic systems usually have more lateral chromatic aberration than symmetrical systems we can expect the Wild to have more color than either the Bausch and Lomb or Olympus microscopes, other factors being equal.

Field of View

The field of view of the microscopes to be compared is limited by a stop in the eyepiece. The angular field in image space was measured (for 10X eyepieces) and found to be $\pm 23^{\circ}$ for the Bausch and Lomb 240, $\pm 25.5^{\circ}$ for the Olympus SZ III, and $\pm 24^{\circ}$ for the Wild M-5. In object space the angular field is just one tenth of that in image space. The field of view is the intersection of the angular field with the object plane and is characterized by a diameter which is called the field size in this study. As the magnification increases, the field remains constant.

At a given magnification we would expect the Olympus microscope to have a slightly larger field size than either the Bausch and Lomb or Wild microscopes. Conversely, for a constant field size, such as

with these SqWR measurements, we would expect the Olympus microscope to have a higher magnification than the other microscopes. Since the numerical aperture generally increases with magnification, a larger aperture in the eyepiece permits better on-axis performance than would otherwise be possible at that field size. However, the larger aperture yields a larger angular field, and the off-axis performance may be degraded. Thus, by increasing the aperture size in the eyepiece, the on-axis performance (for a constant field size) may improve, but the average off-axis performance will probably suffer. Since the angular fields are nearly the same for the microscopes, any performance variations caused by the differences in angular field are probably overshadowed by the effects of gross variations in the numerical apertures and aberrations.

The microscopes were compared at a constant field size which could be adjusted by varying the magnification. Since the Wild M-5 is the only microscope without continuously variable magnification, all the microscopes had to be tested at the Wild's field sizes. This favors the Wild slightly because it is working at supposedly optimized magnifications, while the Bausch and Lomb and Olympus probably are not optimized at those magnifications. The field sizes at which the SqWR was measured are 4.0, 8.1, 16.8 and 34.5 mm. These correspond to magnifications of approximately 50, 25, 12 and 6X, respectively.

Numerical Aperture

The numerical apertures of the microscopes were measured using the principle of the Cheshire Apertometer (Barnard and Welch 1936). This

method is illustrated in Figure 6. A meter stick is placed outside of the object plane of the microscope, and a small aperture is placed on-axis in the object plane. The meter stick is geometrically projected (as if by a pinhole camera) into the entrance pupil of the microscope and then imaged into the exit pupil of the microscope. If the exit pupil is viewed with a small magnifier (10X eyepiece in our case) then the distance BC can be determined immediately. The numerical aperture is given by

$$\text{N.A.} = \sin\theta \quad \text{where } \tan\theta = \frac{BC}{AC} \ .$$

In our case $\theta < 6^{\circ}$, and

$$\text{N.A.} \simeq \frac{BC}{AC} \ .$$

The measured values of the numerical aperture are listed in Table II for each microscope/magnification combination tested. It is interesting to compare the numerical apertures as the magnification of each of the three microscopes is varied from 50X to its maximum value. The N.A. of the Wild microscope increases by 23 percent for a magnification increase of 100 percent (50X to 100X), while that of the Bausch and Lomb microscope increases by 7 percent for a magnification increase of 12 percent (50X to 60X). Finally, the N.A. of the Olympus microscope does not increase at all for a magnification increase of 62 percent (50X to 80X). Thus, the Olympus microscope suffers from empty magnification, and no additional detail is resolved in the top 45 percent of

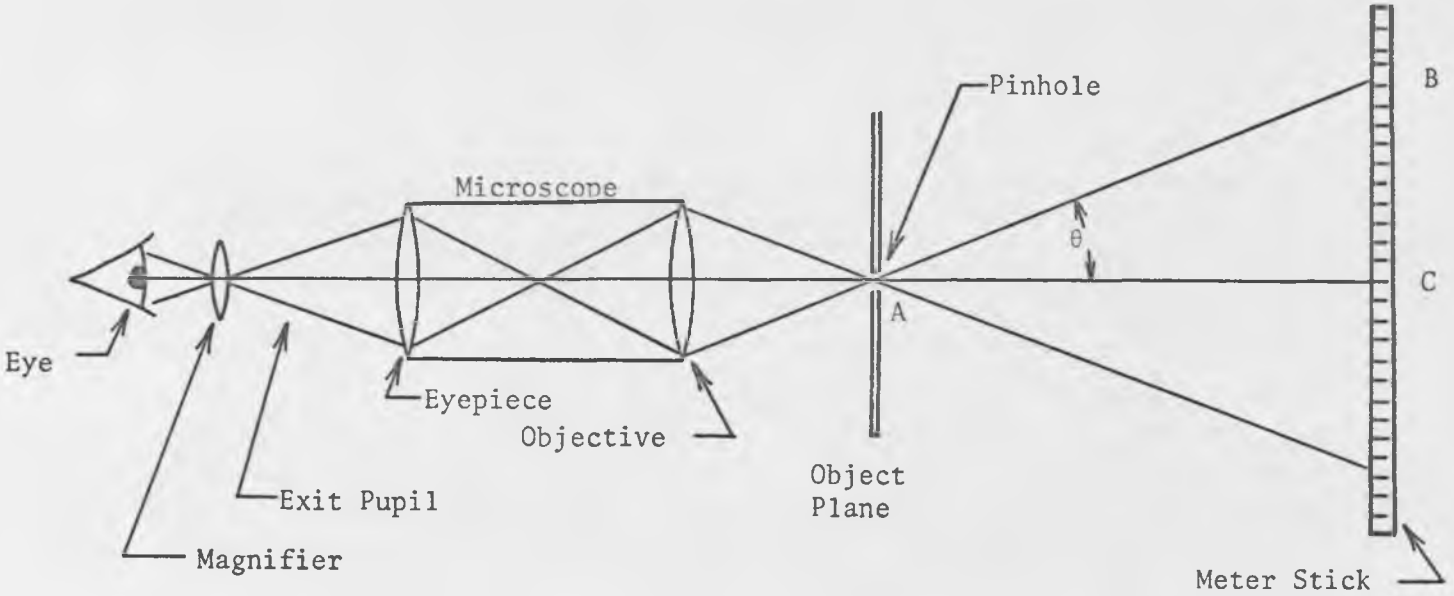

$$\text{N.A.} = \text{Sin}\theta \text{ where } \tan\theta = \frac{BC}{AC}$$

Fig. 6. Measurement of the Numerical Aperture of a Microscope

Table II. Measured and Calculated Characteristics of the Microscopes

Field Size (mm)	Microscopes	Numerical Aperture	Cutoff Frequency, f (cycles/mm)	Depth of Focus d_E (mm)
34	B/12/0.5	.021	77	7.61
	O/13/0.5	.019	71	7.16
	W/6/1	.022	83	7.97
	W/12/05	.022	80	7.87
17	B/12/1	.042	154	1.83
	B/25/0.5	.040	147	1.93
	O/13/1	.043	156	1.76
	O/27/0.5	.039	144	1.66
	W/6/2	.044	162	1.87
	W/12/1	.048	175	1.83
	W/25/0.5	.033	120	2.10
8	B/12/2	.093	339	.463
	B/26/1	.081	296	.463
	O/13/2	.086	313	.454
	O/27/1	.078	284	.432
	W/12/2	.090	328	.468
	W/25/1	.066	243	.523
	W/50/0.5	.040	147	.735
4	B/25/2	.158	575	.122
	O/27/2	.159	580	.106
	W/25/2	.131	477	.132
	W/50/1	.083	302	.179
Minimum				
3.3	B/30/2	.170	620	.088
2.9	O/40/2	.159	580	.060
2.2	W/50/2	.161	585	.046

Microscope Designation

Letter - B = Bausch & Lomb; O = Olympus; W = Wild
First Number - Pod/Eyepiece Magnification
Second Number - Auxiliary Objective Magnification

its zoom range (assuming an aberration free system). In the presence of aberrations, however, the empty magnification may be masked by an improvement in the aberration correction.

Diffraction-Limited Cut-Off Frequency and Depth of Field

The Abbe treatment of microscope imaging predicts that the diffraction-limited cut-off frequency, f, is given by (Carpender 1969, p. 31)

$$f = \frac{(N.A.)_L + (N.A.)_I}{\lambda} ,$$

where $(N.A.)_L$ and $(N.A.)_I$ are the numerical apertures of the objective and condenser respectively, and λ is the wavelength of the light. For incoherent illumination $(N.A.)_L = (N.A.)_I$, and

$$f = \frac{2\ (N.A.)_L}{\lambda} . \qquad (5)$$

The cut-off frequencies were calculated for the measured values of numerical aperture (for λ = 555 nm) and are listed in Table II.

For a microscope at a particular magnification, the cut-off frequency is higher when using auxiliary objectives of greater magnification. For example, if the magnification of a microscope is doubled by adding a 2X auxiliary objective, the N.A. and cut-off frequency also double. However, if the magnification of the microscope is doubled by changing the pod magnification, the N.A. and cut-off frequency increase by a factor less than two. Similarly, the 0.5X auxiliary objective

halves the microscope magnification and the cut-off frequency; but if the pod magnification is halved, the cut-off frequency is reduced by a factor less than one half. Thus, the maximum diffraction-limited cut-off frequency is obtained at a given magnification by using the highest possible auxiliary objective magnification.

The geometric depth of focus, d, of a microscope is expressed as (Benford 1965, p. 6)

$$d = \frac{\lambda\,[n^2 - (N.A.)^2]^{\frac{1}{2}}}{(N.A.)^2} \quad ,$$

where λ is the wavelength of light, n is the index of refraction in object space (n = 1 in this study), and N.A. is the numerical aperture of the objective. For numerical apertures less than 0.2, $[1-(N.A.)]^2 \simeq 1$ to within 2 percent, and

$$d = \frac{\lambda}{(N.A.)^2} \quad .$$

If the microscope is being used visually, the effective depth of focus is greater than d because of the eye's ability to accommodate. Assuming the eye can accommodate to 250 mm, the effective depth of focus d_E, of a microscope with magnification M is given by

$$d_E = \frac{\lambda}{(N.A.)^2} + \frac{250}{M^2} \quad , \qquad (6)$$

where λ and d_E are expressed in millimeters. Calculated values for d_E are given in Table II for the magnifications and numerical apertures used in this study.

At high numerical apertures and magnifications, the depth of focus is very small. If the numerical aperture is increased further, the cut-off frequency will increase linearly, but the depth of focus will decrease quadratically. Thus, when we increase the N.A. of a microscope in order to improve its performance, we must accept a large decrease in its depth of field. This places a burden on the film flattening and hold down techniques used on photointerpretation equipment, and at high magnifications the inadequacies in the film flattening techniques may limit the usable N.A. of the microscope. However, in this study the depth of focus will not be a criterion of comparison since we are concerned with the performance of the microscope when viewing perfectly flat imagery located in the object plane of the microscope.

The Effects of Converging Optical Channels

The object plane of the microscope shown in Figure 5 is not normal to either optical axis, but is tilted approximately 1^0, 2.5^0, and 5.5^0 from the geometric plane of best focus for the 0.5X, 1X and 2X auxiliary objectives, respectively. That is, the angle between the optical axes is about 2^0, 5^0 and 11^0, depending on the auxiliary objective used. These angles vary only slightly between microscopes. As a result, the left and right sides of the image, as viewed from the normal operating position, are out of focus. Since the 2X auxiliary objective produces the largest tilt and the smallest depth of focus (see Table II), with this objective we can expect rapid deterioration

of the image quality as we move off-axis to the left or right. With the 0.5X auxiliary objective the tilt is less and the depth of focus greater, so the off-axis positions will not be as badly out of focus. Thus, at a given magnification the image quality with the 0.5X auxiliary objective should be more nearly constant over the field than with either of the other auxiliary objectives (for an aberration free system).

The introduction of field curvature into the aberration free microscope can produce interesting results (see Figure 7). On the left side of the field (position A) the surface of best focus has curved towards the object plane, while on the right side (position B) it has curved away from the object plane. The result is an improvement in image quality at A, but a deterioration at B. Therefore, when viewed through the right optical channel, the right side of the field is in best focus, while through the left channel, the left side is in best focus. The manner in which the human visual system superimposes these two different images is of interest, but lies outside the scope of this study.

Field curvature is not the only aberration which can cause one side of the image to be in better focus than the other side. Astigmatism could improve the focus of image elements in a certain orientation for one side while degrading the focus on the other side of the field. Also, there are probably non-axially-symmetric effects caused by the cycloptic auxiliary objectives.

The intention of this discussion is not to provide a complete and detailed analysis of microscopic imaging from a tilted object plane.

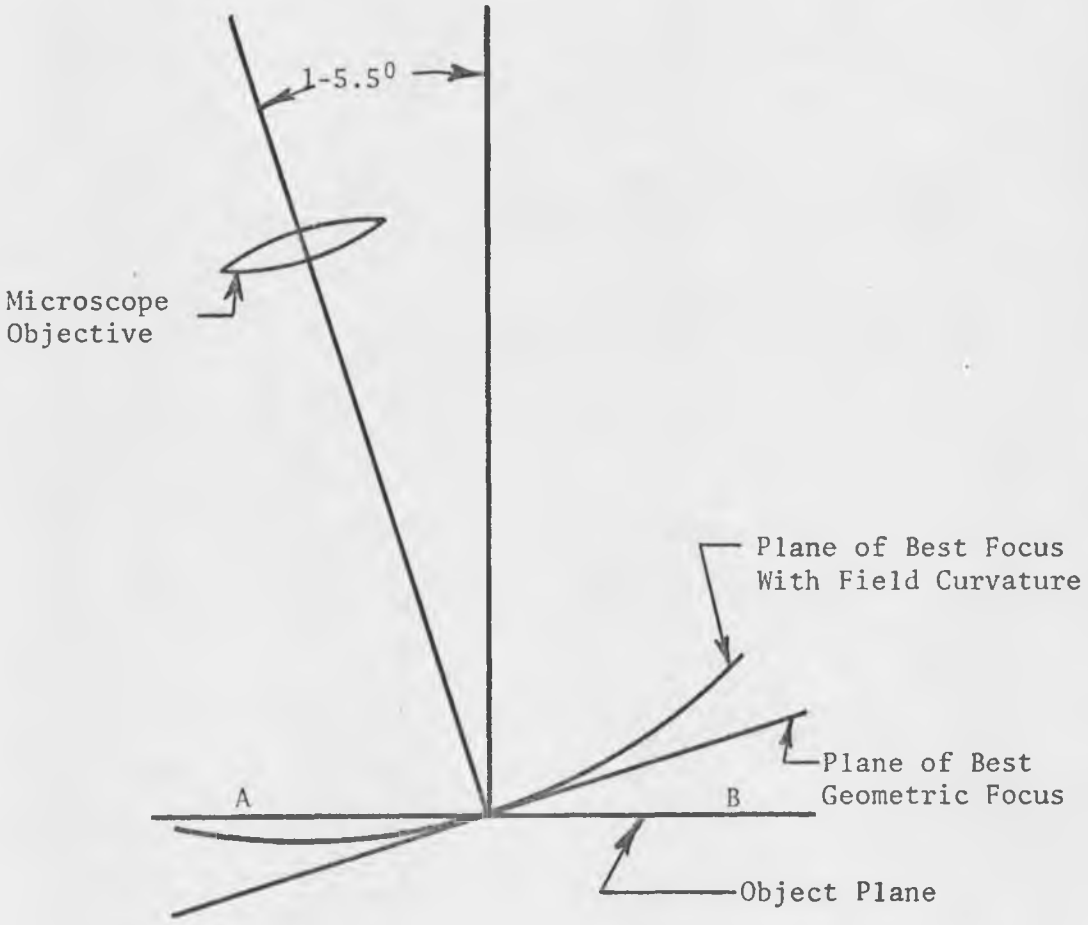

Fig. 7. Possible Effect of Field Curvature on the Tilted Object Plane

Rather, we want to illustrate that peculiar effects may be observed in the images and SqWR of stereomicroscopes because of the tilt. In particular, off-axis performance at certain field points (in the neighborhood of position A) may be as good as, and perhaps better than, on-axis performance.

Scattered Light

Scattered light (or flare) reduces the contrast and modulation of a microscope image. If the irradiance of the scattered light is denoted by S, then the modulation of the image is reduce to

$$M = \frac{I_{max} - I_{min}}{I_{max} + I_{min} + 2S} \quad . \tag{7}$$

There are three primary sources of scattering in microscopes: (1) multiple reflections off the glass surfaces, (2) reflections off the lens ridges and (3) reflections from mechanical parts, such as cell walls.

With diffuse illumination, such as from a light table, the scattered light can originate inside or outside of the field of view. By placing an aperture in the film plane that allows only a small portion of the field to be transmitted, the modulation can be increased by 0.1 modulation units over a large range of spatial frequencies (Anseley and Cykowski 1968). However, it is not usually desirable to reduce the field of view, and in practice it would be difficult to block the light coming from outside the field of view. Thus, scattered light is present in the images formed by the microscopes, and its effects were included, as they should be, in the SqWR measurements.

The average density of the imagery in the object plane of the microscope influences the amount of light entering the microscope, and hence, the amount of light which is scattered. With imagery of a low average density, more light will be transmitted to the microscope and scattered than with imagery of high average density. The average density depends on the subject matter of the imagery, as well as on its contrast.

Similarly, when measuring the SqWR, the amount of scattered light in the image of the test target depends on the average density of the test target and its position and orientation in the object plane. This is unfortunate since we would like the amount of scattered light to be independent of the test target position and orientation in the field. However, the variations in scattering were not significant at the field sizes used in this study, and they caused a variation of less than 4 percent in modulation for most cases.

The Influence of the Eye

The microscopes in this study are used as visual instruments and, therefore, a comparison of their optical performance should include how well they present an image to the eye. In particular, the microscopes should magnify the image sufficiently so that the eye can easily resolve the highest frequency components that are resolved by the microscope. Thus magnification is one of the three criteria mentioned in Chapter 1 that are being used to compare the microscopes.

Each microscope has sufficient magnification to make its exit pupil less than 2 mm in diameter (1.8 mm for the Bausch and Lomb and

Olympus; 1.9 mm for the Wild). This means that the effective aperture of the eye, when positioned in the exit pupil of the microscope, is just the size of the exit pupil. Since the eye pupil is never smaller than 2 mm, and is nearer 4-5 mm for microscopic viewing, the eye does not introduce significant image degrading diffraction effects. In addition, the aberrations of the eye are small compared to diffraction effects for pupil diameters less than 2 mm, and thus eye aberrations, as well as diffraction effects, do not limit the cut-off frequency of the eye/microscope combination. It is the microscope which determines the cut-off frequency, although the eye lens may modify the modulation of frequency components which are less than the cut-off frequency.

The retina is able to resolve about 1.0 cycles/minute of arc near the fovea, and the magnification of the microscope is sufficient to make the maximum frequency component in the microscope image about 0.5 cycles/minute of arc. Thus, the retina can resolve the microscope image, provided the image modulation is sufficient (greater than 0.025, typically). Unfortunately, the effect of the retina on the image modulation is much more difficult to predict since there are many variables which can influence the SWR and SqWR of the eye.

Nevertheless, all three microscopes present images to the eye which can be resolved because the images have been magnified sufficiently. Therefore, magnification is not a distinguishing characteristic of the information transfer, and only SqWR and field of view need to be used for the comparison.

CHAPTER 4

DETERMINING THE SQUARE WAVE RESPONSE

The Apparatus

The square wave response of the microscopes was determined by scanning a square wave test target in the object plane of a microscope and measuring the irradiance variations at a particular point in the image plane. The configuration of the equipment used to make the measurements is shown in Figure 8, and a photograph of the equipment is shown in Figure 9. The apparatus consists of four functionally separate stages: (1) an illumination stage, (2) a target stage, (3) a microscope stage and (4) a detection stage. Each of these will now be described and its influence on the square wave response discussed.

The Illumination Stage

The light source was a 500 watt tungsten projection lamp that was operated at 90 VAC (corresponding to a color temperature of 3080^{o}K). The lamp filament was located in the front focal plane of condenser element A and at the center of curvature of a spherical reflector positioned behind the lamp (see Figure 8). Lens A collected (relative aperture f/1.5) and collimated the light, which then illuminated the field stop, S_1.

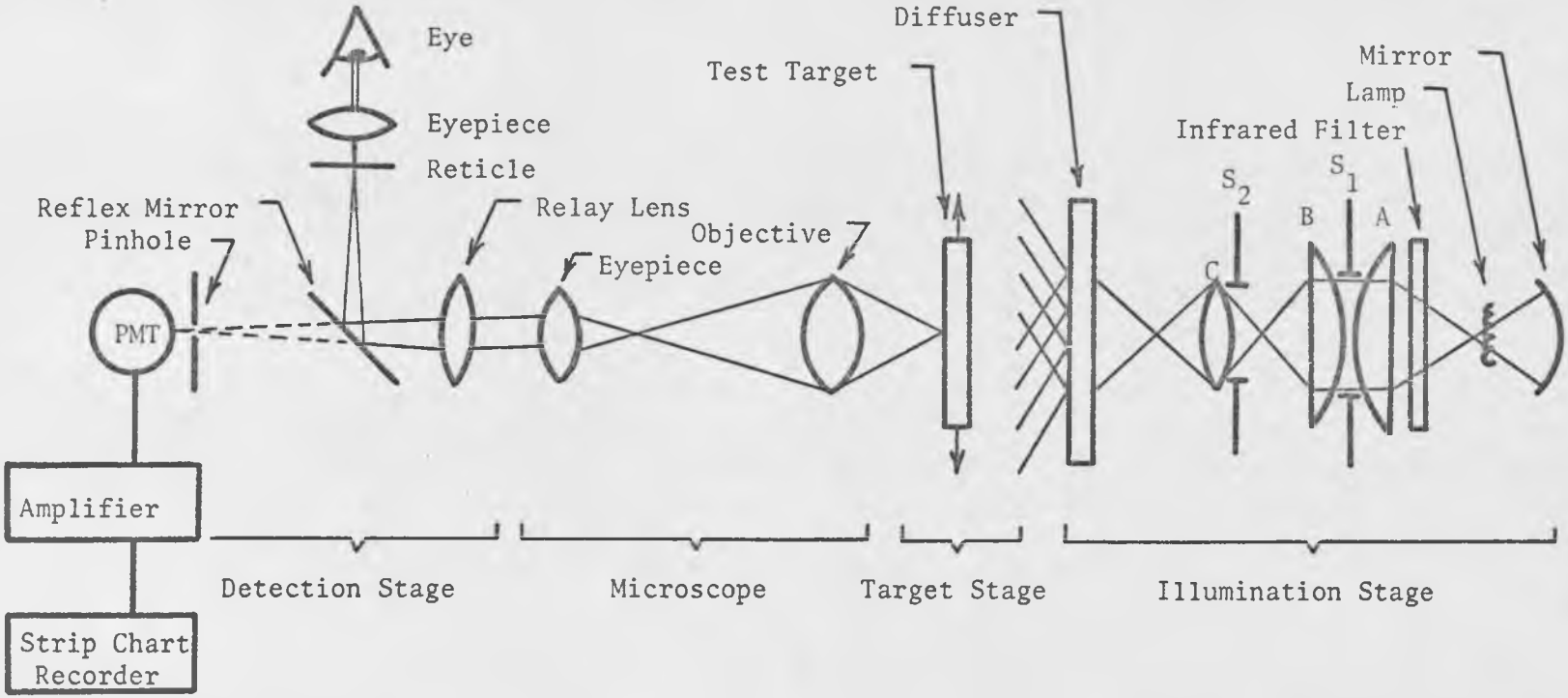

Fig. 8 Configuration of the SqWR Measuring Equipment

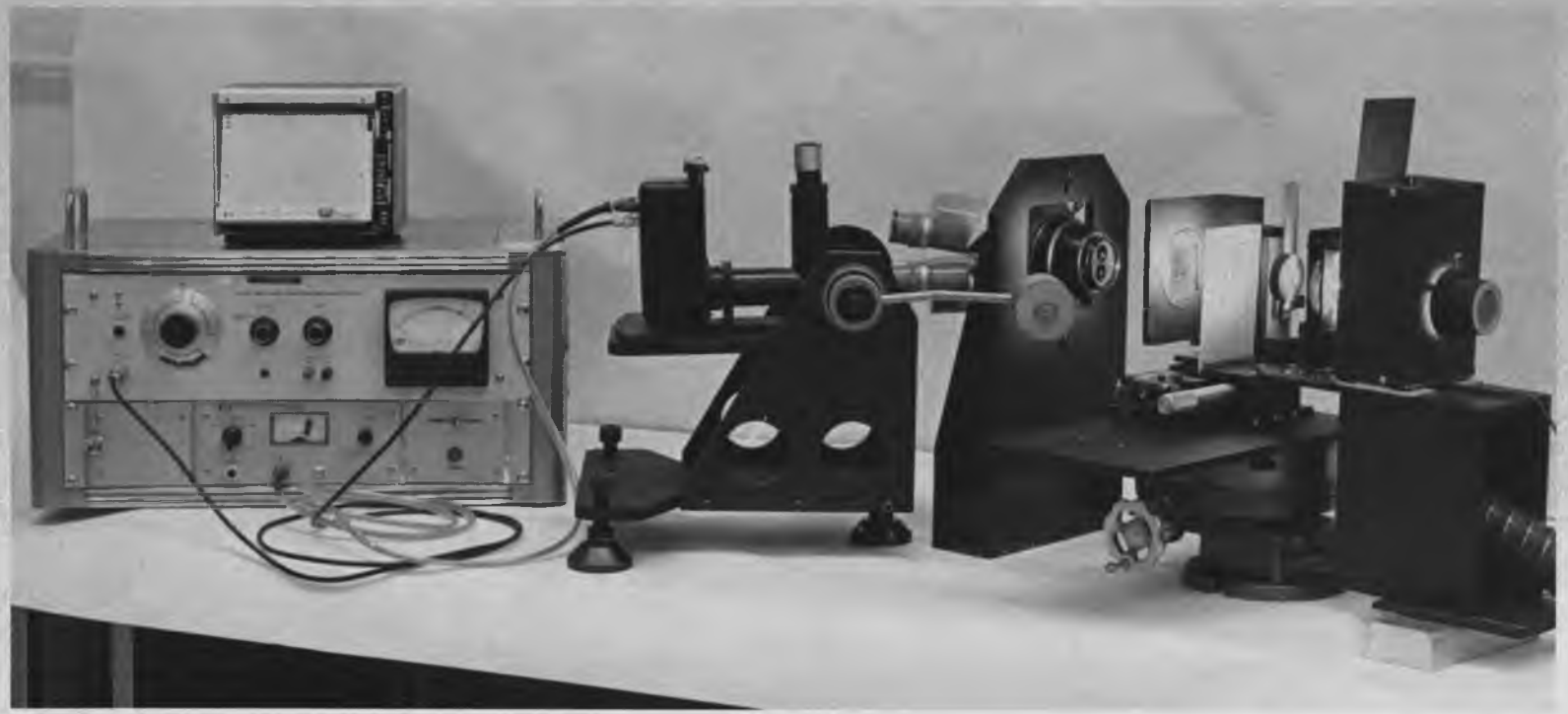

Fig. 9. The SqWR Measuring Equipment

The image of the filament formed in the rear focal plane of condenser lens B and was 1.36 cm across its diagonal, or about 1.15 times larger than the actual filament. Lens C and the aperture stop, S_2, were also located in the rear focal plane of lens B and imaged field stop, S_1 onto the diffuser. The size of the image of S_1 could be changed by varying the size of S_1 or by varying the focal length of lens C. For a focal length of 17 mm, and with S_1 fully opened, the image diameter was 1.3 cm. The brightness of the image could be varied with the aperture stop, S_2; hence a change in the brightness could be made without changing the voltage of the lamp and, consequently, its color temperature.

The function of the illumination stage was to illuminate the test target in the same manner that a light table illuminates aerial imagery. In this way, the microscopes could be tested under the same conditions for which they are normally used. Typically, a light table consists of a large fluorescent-tube grid which illuminates a plastic diffuser (a common diffuser size is 10 x 30 inches). The plastic diffuser is positioned from 0.25 to 2 inches (depending on the particular light table) under a clear glass plate which supports the aerial imagery. The illumination stage was effectively equivalent to this type of light table.

The qualities of the illumination source that are of concern are its size, coherence and spectral characteristics. The size of the effective source directly influences the amount of scattered light in

the image. A light table has a very large effective source and may therefore contribute scattered light from both inside and outside the field of view. Since we expect that most of the scattered light will come from areas within the field of view, the image of S_1 on the diffuser should be at least as big as the microscope field size. For the SqWR measurements, the source size was about twice as large as the field size.

The degree of coherence of the illumination in the object plane will have a great influence on the response characteristics of a microscope. It is important, therefore, that the microscope be tested with illumination of the same coherence as found on light tables. Hopkins (1957) has shown that the illumination is effectively incoherent, over all dimensions of interest, if the numerical aperture (N.A.) of the condenser is at least 2.5 times greater than the numerical aperture of the microscope objective. He stresses that this is not a rigid requirement, and even if the numerical apertures are equal only "poor coherence" will exist between resolved points.

The largest N.A. of any of the microscopes in this study is 0.18. Thus, to have incoherent illumination the N.A. of the condenser must be approximately 0.45, or greater. Since the illuminated area on the light table is so large, the N.A. associated with the light table is much larger than 0.45, and the light table incoherently illuminates the object plane of the microscope. The numerical aperture of the condenser in the SqWR equipment is found by dividing the diameter

of the image on the plastic diffuser by twice the distance from the diffuser to the object plane. When the microscope is at its highest magnification, the N.A. of the condenser is 0.37. Therefore, the illumination stage also provides light that is effectively incoherent in the object plane.

The spectrum is the final characteristic of the illumination to be considered. On a light table the imagery is illuminated by a fluorescent source, and the microscope forms an image which is detected by the eye. The spectrum of the fluorescent light, when weighted by the response of the eye, is the effective spectrum of the image forming light. This effective spectrum is closely matched in the SqWR equipment by using an S-1 photocathode to sense a tungsten source at 3080°K. Therefore, the microscopes are being tested with light of the same range of wavelengths as found in an operational situation.

The SqWR equipment employs white light illumination because the microscopes are used with white light. However, the theory of SWR usually is developed for monochromatic light, and the SWR is measured using nearly monochromatic light. Even so, there is no fundamental reason that disallows a white light SWR, and in fact Köhler and Metzmacher (1969) have used the white light SWR to describe the degree of color-correction of an optical system.

The Target Stage

The test target was manufactured by Diffraction Limited and consists of thirty high-contrast (contrast > 2) square wave patterns

on a two-inch-square glass slide. The patterns themselves consist of transparent bars on an opaque background and are arranged in three groups. The first two groups contain eleven patterns and the third group contains eight patterns. The spatial frequencies (in line pairs/mm or cycles/mm) of the patterns are given in Table III.

Figure 10 shows photomicrographs of the test target. At a low magnification of 14.4X (Figure 10a) all of the patterns in groups 2 and 3 can be seen, but most patterns in group 1 are excluded from the picture area. At a high magnification of 119X (Figure 10b) only the patterns in group 3 are totally included.

An important feature of the test target is that each square wave pattern has fifteen cycles. Barakat and Lerman (1966) have calculated that for incoherent illumination a seven cycle square wave target effectively approximates a square wave of infinite extent. They caution, however, that the modulation should be calculated near the center, not at the ends, of the target. Therefore, the fifteen cycle square wave pattern used for measuring SqWR is effectively an infinitely long square wave. Since SqWR and SWR are defined in terms of infinite waves, the data obtained with the fifteen cycle patterns can be converted to SWR using Equation (4). Such a conversion could not validly be made with results from a three cycle target. Another advantage of the fifteen cycle target over a three (or even a seven) cycle target is that it allows us to average over a greater number of cycles when calculating the modulation.

Table III. Spatial Frequencies (cycles/mm) of the Square Wave Test Patterns

Element	Group 1	Group 2	Group 3
1	1.00	10.0	100
2	1.26	12.6	126
3	1.58	15.8	158
4	2.00	20.0	200
5	2.51	25.1	251
6	3.16	31.6	316
7	3.98	39.8	398
8	5.01	50.1	501
9	6.31	63.1	
10	7.95	79.5	
11	10.00	100	

a. 14.4X Magnification

b. 119X Magnification

Fig. 10. The Square Wave Test Target

The test target was mounted on a x-y-z stage movement. The x-y movement was oriented in a plane normal to the optical axis of the condenser. Two functions were performed by the x-y movement: (1) the target could be placed at various positions in the microscopes field and (2) the test target could be scanned across the field position. Micrometers with two-inch movements were used to drive the target in the x and y directions. The z-axis was parallel to the optical axis of the condenser and movement along this axis enabled proper focusing of the test target in the object plane of the microscope.

The SqWR measurements were made by manually scanning the test target across a given field position in the x or y directions. Since the only concern was with the maximum and minimum values of irradiance in the image, the scanning motion did not have to be extremely linear. The only advantage in having a linear scan was that we could then perform some averaging when trying to determine a particular irradiance level on the strip chart recording. For most of the measurements the micrometers could be driven by hand in a smooth, linear scan.

As frequency of the square wave pattern increased, the problems associated with scanning increased. At high frequencies the scan rate had to be decreased since the chart recorder has a fairly long response time (.25 second, full scale deflection). The minimum scan rate was approximately one square wave cycle per second, or 20μm/second for the pattern of the highest frequency. In addition, vibrations from the operators hand on the micrometer at times produced an erratic scanning motion. As a result, the output signals from scanning high frequency

patterns were often noisy, and if the signals were low, they at times could not be detected or accurately measured. Surprisingly, however, if extreme care was exercised in scanning, measurements could be made at 500 cycles/mm.

The Microscope Stage

The microscopes were mounted horizontally in a massive structure to minimize vibration. The mounting was such that the left channel of each microscope (as viewed from a normal operating position) was tested.

The microscopes were tested with the virtual images located at infinity. Often microscopes are designed to be used with the virtual image at 25 cm distance, the near point of distinct vision. However, photointerpreters spend long hours looking into microscopes and focus them for the least fatiguing image. Since the relaxed eye focuses at infinity, the least fatiguing focus will be for the image at infinity.

The Detection Stage

The detection stage sensed and recorded the image irradiance at a particular field position of the microscope. It consisted of a lens which relayed the virtual image of the microscope to a pinhole. The pinhole in turn sampled a portion of the image, and the irradiance of that portion was sensed by the photomultiplier tube (PMT). The relay lens, pinhole and PMT were mounted on a gimballed assembly which permitted the selection of the field position to be viewed.

Since the microscope was focused to form its image at infinity, the light leaving the eyepiece was collimated. This collimated beam was collected by the relay lens, a well-corrected telescope objective (focal length = 133 mm; diameter = 15 mm) whose entrance pupil was positioned in the exit pupil of the microscope. The entrance pupil of the relay lens was much larger than the exit pupil of the microscope (15 mm vs. 1.8 mm), and thus there was no image degradation caused by diffraction at the relay lens.

The aberrations introduced by the relay lens were also negligible. Telescope objectives are highly corrected for a small field near the optical axis. The sampling pinhole was located on the optical axis and limited the effective field of the telescope to its optimum, on-axis position. In addition, only the center portion of the telescope objective was used due to the small size of the exit pupil of the microscope. This minimized any on-axis aberrations which may have been present. Therefore, the telescope objective should not have significantly degraded the virtual image of the microscope in transferring it to the plane of the pinhole.

The gimballed mount rotated the relay lens, pinhole and PMT about the exit pupil of the microscope. For any orientation, the center of the exit pupil of the microscope and the entrance pupil of the relay lens were coincident (see Figure 11). By rotating this assembly, all portions of the microscope field could be viewed on the optical axis of the relay lens. Thus, there is negligible image degradation due to the relay lens for all microscope field positions.

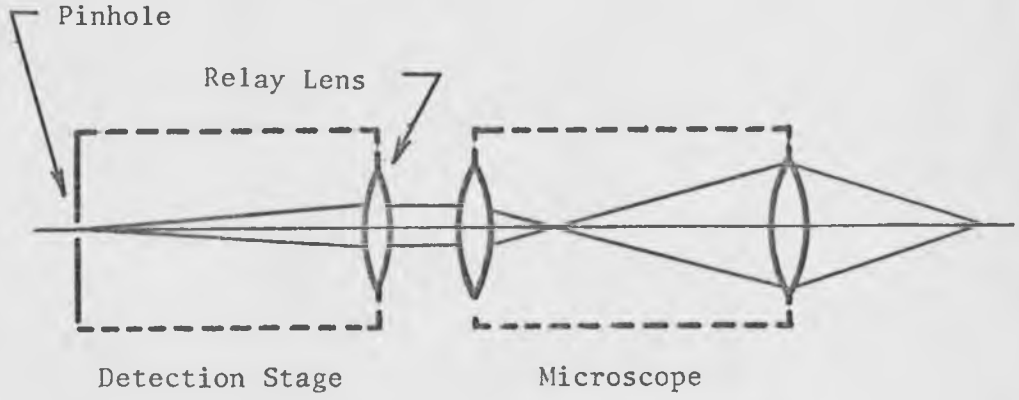

a. On-Axis Position

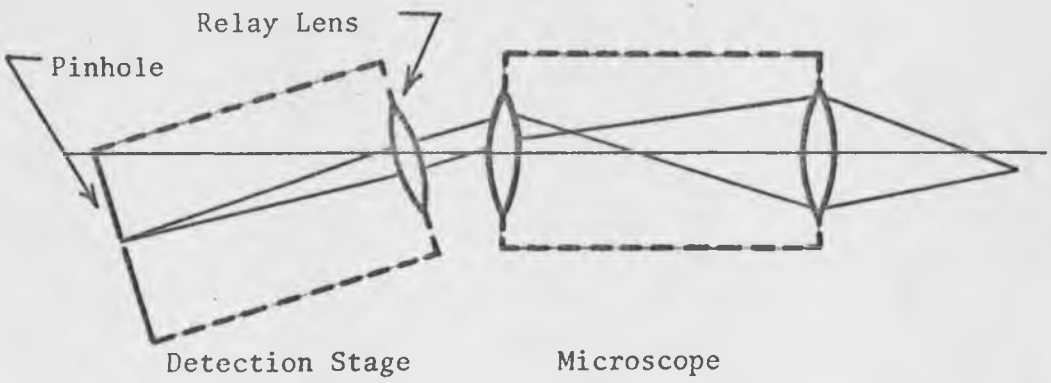

b. Off-Axis Position

Fig. 11. Viewing Different Microscope Field Positions with the Detection Stage

The pinhole, which was located in the focal plane of the telescope objective, sampled the image. It was necessary that the pinhole be sufficiently small so that the image detail would not be lost. Using the criteria (from microdensitometry) that the pinhole should be no larger than 1/6 the size of the smallest square wave pattern imaged on it, the maximum size of the pinhole should be 11μm. A 10μm pinhole was used.

The PMT (type 1P21) sensed the irradiance transmitted by the pinhole and produced a proportional signal which was sent to a Keithley Model 414 Micro-microammeter. The amplified signal from the ammeter was displayed on a Mosely 680M Strip Chart Recorder. A typical output of the strip chart recorder for an entire SqWR measurement is shown in Figure 12.

The photomultiplier and amplifier were calibrated by measuring the amplifier output as a function of illumination on the PMT. The combination was linear over six decades of PMT inputs, including the region where the SqWR measurements were made.

While a PMT has a particular spectral response, it can not distinguish between colors as can the eye. The PMT does not sense color, but only the irradiance of the light as weighted by the spectral response of the PMT. Thus, if a microscope suffers from chromatic aberration, the PMT would not sense the color, but only the weighed irradiance of the image. On the other hand, the eye would see a colored image, possibly a series of red and blue bars if a square wave target were viewed. We

might then say that the eye can resolve the square wave pattern better than the PMT. This is true if the object is simple, such as a square wave pattern. However, if a complex image is synthesized from many sets of square waves, then the value of the color information is lost; the colors are "jumbled" together. Thus, the SqWR obtained here is such that it may be used in evaluating a microscope's response to the complex objects commonly found in aerial imagery.

The detection stage had a reflex viewing system which permitted the image of the test target to be focused accurately on the pinhole. The image was in focus only if collimated light entered the relay lens. In order to focus (see Figure 8), a reflex mirror was placed behind the relay lens such that the light was directed upwards to a reticle located in the focal plane of the relay lens. When collimated light entered the relay lens, the image of the test target was superimposed on the reticle, and both test target and reticle appeared in focus when viewed with an eyepiece. Once the position of the test target was adjusted to bring both the reticle and the test target into focus, the reflex mirror was withdrawn, and a properly focused image appeared in the plane of the pinhole.

The Measurements

The SqWR was measured at the field sizes and corresponding magnifications, given in Table II (Chapter 3). There were four field sizes common to all three microscopes, and these formed the basis for

comparison. Twenty-one microscope/lens combinations produce these field sizes, and all were tested. In addition, the SqWR at the maximum magnification of each microscope was measured.

For each field size, seven or eight SqWR curves were made. The curves included one on-axis position and three off-axis positions for both radial and tangential orientations of the test target. In some cases two on-axis SqWR curves were made because the on-axis SqWR seemed to depend on the test target orientation.

The field positions for which SqWR curves were made are shown in Figure 13. This figure shows the field when viewing through the left eyepiece with the microscope in its normal operating position. If the two optical channels are symmetric, then the view through the right eyepiece would have positions 3 and 4 interchanged. Notice that when viewing through the left-eyepiece, position 3 corresponds to position B and position 4 corresponds to position A in Figure 7. We would expect these positions to have different SqWR curves. However, due to symmetry, position 2 and the diametrically opposing position should have nearly the same SqWR. This was experimentally verified in several cases, and thus only the SqWR at position 2 was measured for the comparison in this study.

The lines drawn through the field positions in Figure 13 show the test target bar orientation for a particular SqWR curve. The letter after the field position designator number indicates a radial (R) or tangential (T) target orientation. For example, a SqWR curve

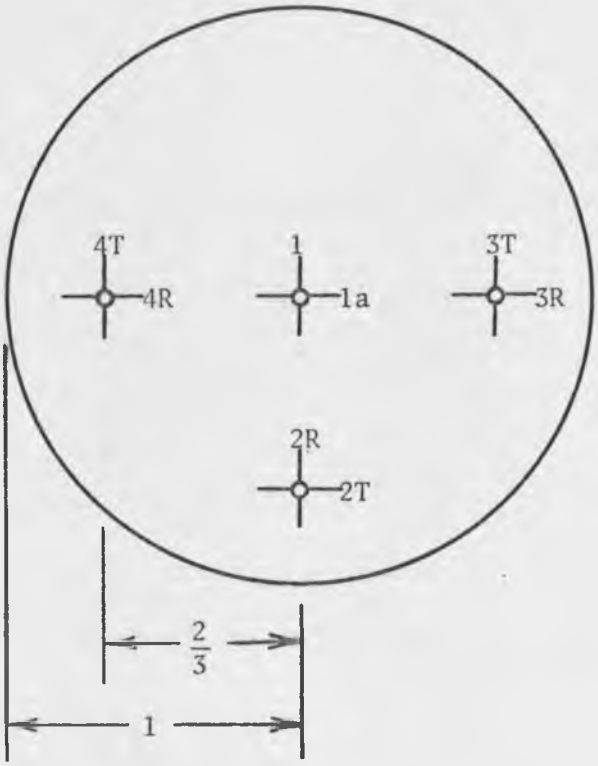

Fig. 12. Microscope Field Positions at which the SqWR was Measured

designated by 4T was made at position 4 with a tangential target orientation. This designation will be used in the next chapter to identify the SqWR curves plotted for each field size.

For each set of SqWR curves, the microscope under test was focused for maximum on-axis resolution (for orientation 1, not 1a). When the SqWR for off-axis positions was measured the microscope was not refocused. This procedure is somewhat arbitrary in two respects. First, the focal position for maximum on-axis resolution does not necessarily correspond to that for the best overall SqWR. At different focal positions the aberrations may offset one another such that the response is very high out to a frequency that is less than the maximum on-axis frequency. However, any criterion other than maximum resolution would require many additional SqWR measurements, which was outside the scope of this program.

Secondly, by not refocusing the microscope for off-axis positions we are neglecting the ability of the eye to accommodate. That is, off-axis performance may appear better visually than the SqWR curves indicate because the eye can accommodate to a certain extent and perhaps bring the off-axis image into focus. Unfortunately, the amount of possible accommodation varies considerably between individuals, and it is not known if even the "average" accommodation is sufficient to bring a particular off-axis position into focus. Therefore, since the SqWR curves were made without refocusing off-axis positions, these curves represent a "worst-case" condition for visual observation. They are realistic, however, for photomicrographs taken through the microscopes.

The Calculations

The strip chart recording shown in Figure 12 constitutes the raw data for one SqWR curve. Patterns of at least ten different spatial frequencies were scanned for each curve. This data was converted to SqWR by applying Equation (2) which can be written as

$$M = \frac{I_{max} - I_{min}}{I_{max} + I_{min}}$$

Where I_{max} , I_{min} are now averages of the maximum and minimum irradiance values, respectively, associated with each square wave pattern. Since the scale on the strip chart was arbitrary, I_{max} and I_{min} were expressed distances above the base line (I = 0). The modulation for each spatial frequency was found by measuring the distance $(I_{max} - I_{min})$ with a ruler and then dividing it by the sum of the distance $(I_{max} + I_{min})$.

Before these distances were measured, the average minimum and average maximum intensities had to be found for a number of cycles. Heeding the warning of Barakat and Lerman (1966) against using the square waves at the end of the pattern, the averages were found for the ones in the middle. The averages were not obtained mathematically, but rather by visual inspection of the traces.

The error associated with determining I_{max} and I_{min} from the strip chart record and then calculating the modulation is small. The percentage uncertainty in modulation can be expressed as

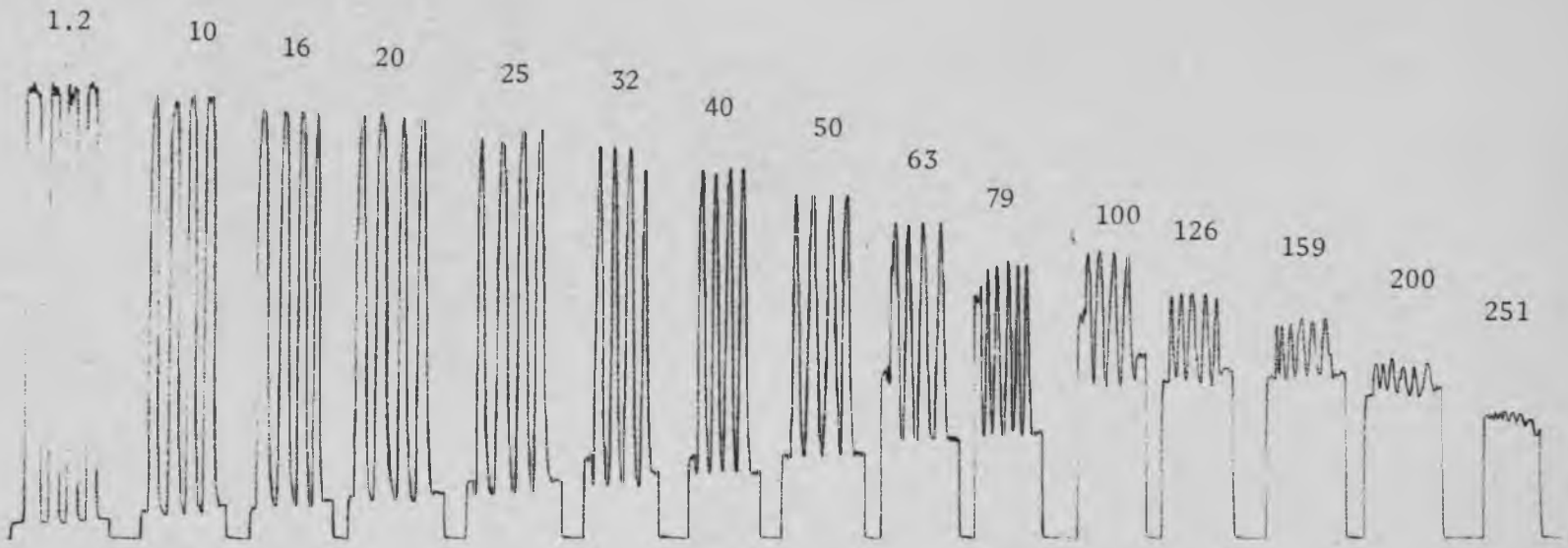

Fig. 13. Typical Strip Chart Record of a SqWR Measurement

$$\frac{\Delta M}{M} = \frac{1+\dfrac{\Delta I_{max} + \Delta I_{min}}{I_{max} - I_{min}}}{1+\dfrac{\Delta I_{max} + \Delta I_{min}}{I_{max} + I_{min}}} - 1 \quad ,$$

where ΔI_{max} and ΔI_{min} are uncertainties in determining I_{max} and I_{min} on the strip chart record. Substituting realistic values for the uncertainties into the expression for $\Delta M/M$ yields the following typical uncertainties.

High Modulation: $\Delta M = \pm 0.004$

$\frac{\Delta M}{M} = \pm 0.5 \quad \%$

Medium Modulations: $\Delta M = \pm 0.010$

$\frac{\Delta M}{M} = \pm 3.5 \quad \%$

Low Modulations: $\Delta M = \pm 0.012$

$\frac{\Delta M}{M} = \pm 8.5 \quad \%$

In the worst case the uncertainty is about ±.01, which is slightly larger than the resolution of the SqWR curves.

CHAPTER 5

THE MEASURED SQUARE WAVE RESPONSE OF THE MICROSCOPES

The SqWR curves of the microscopes are shown in Figures 14-38, and are arranged by the microscope field size: Figures 14-17 for the 34 mm field, Figures 18-24 for the 17 mm field, Figures 25-31 for the 8 mm field, Figures 32-35 for the 4 mm field and Figures 36-38 for the minimum field sizes. Each Figure includes the seven or eight SqWR curves associated with a particular microscope/lens configuration. Each SqWR curve is identified by field position and test target orientation as in Figure 13 (Chapter 4) and each microscope of a particular lens configuration is designated by the notation of Table II (Chapter 3).

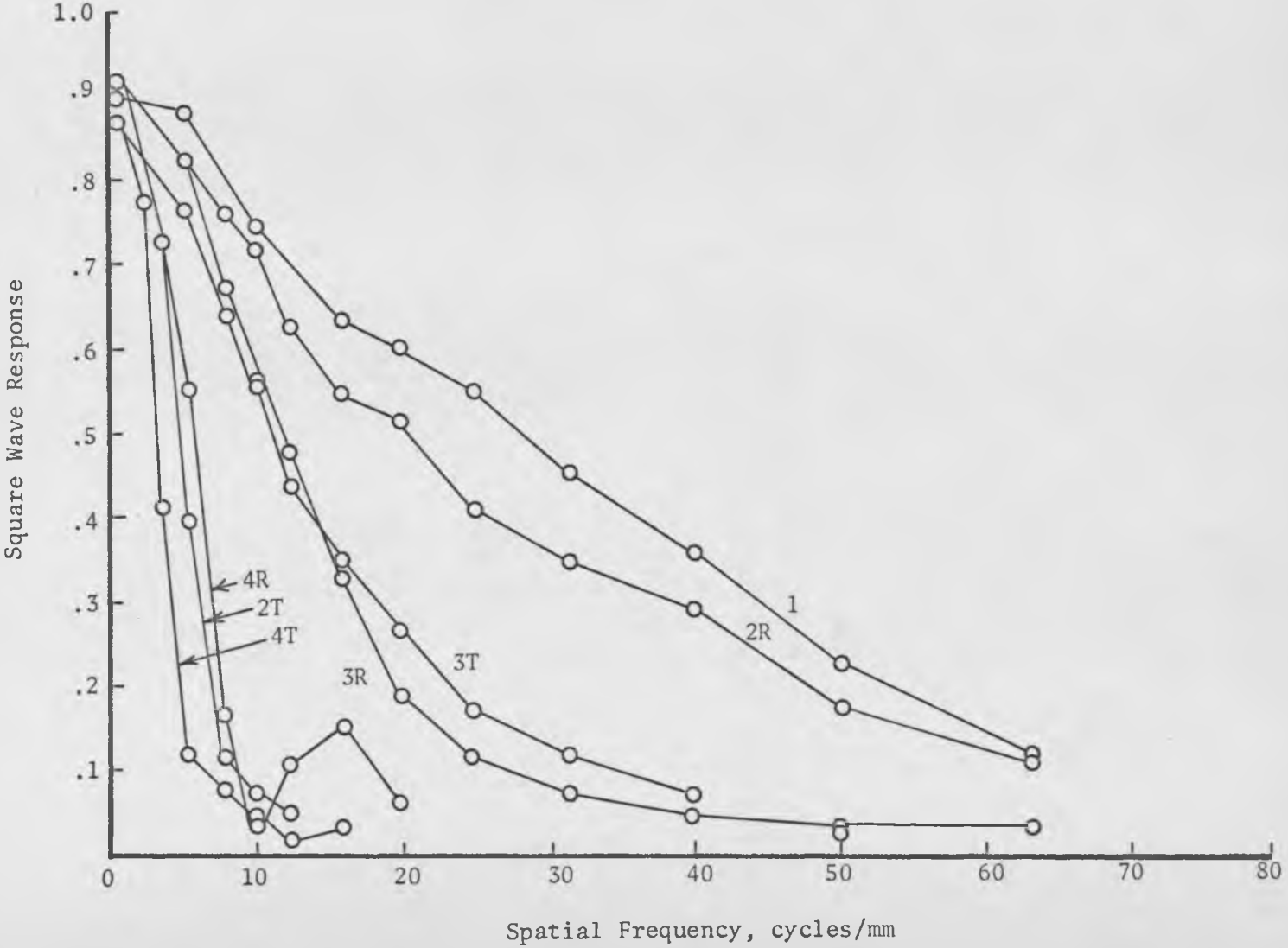

Fig. 14. Square Wave Response of the Bausch & Lomb Microscope (B/12/0.5; 34 mm field)

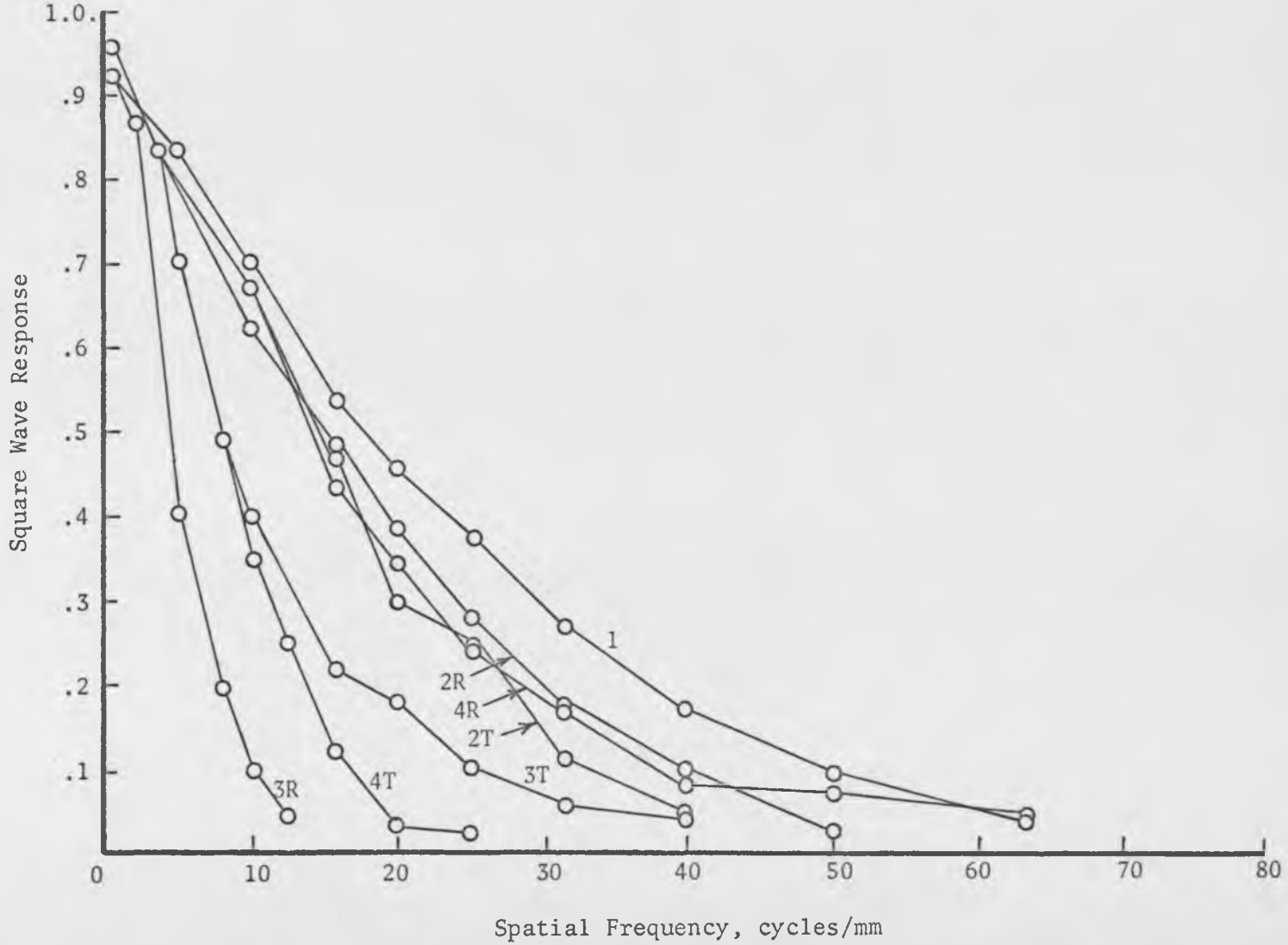

Fig. 15. Square Wave Response of the Olympus Microscope (O/13/0.5; 34 mm field)

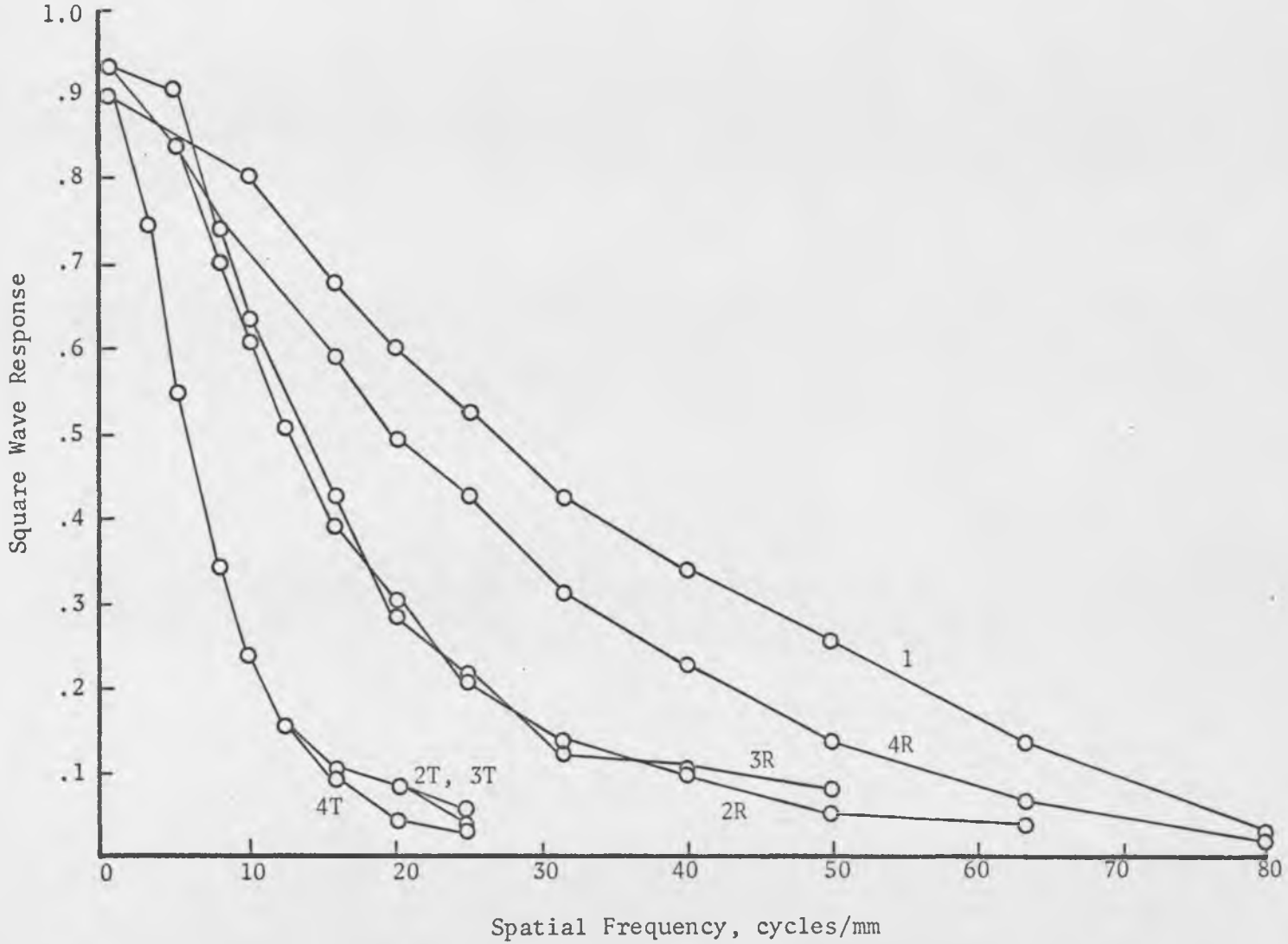

Fig. 16. Square Wave Response of the Wild Microscope (W/6/1; 34 mm field)

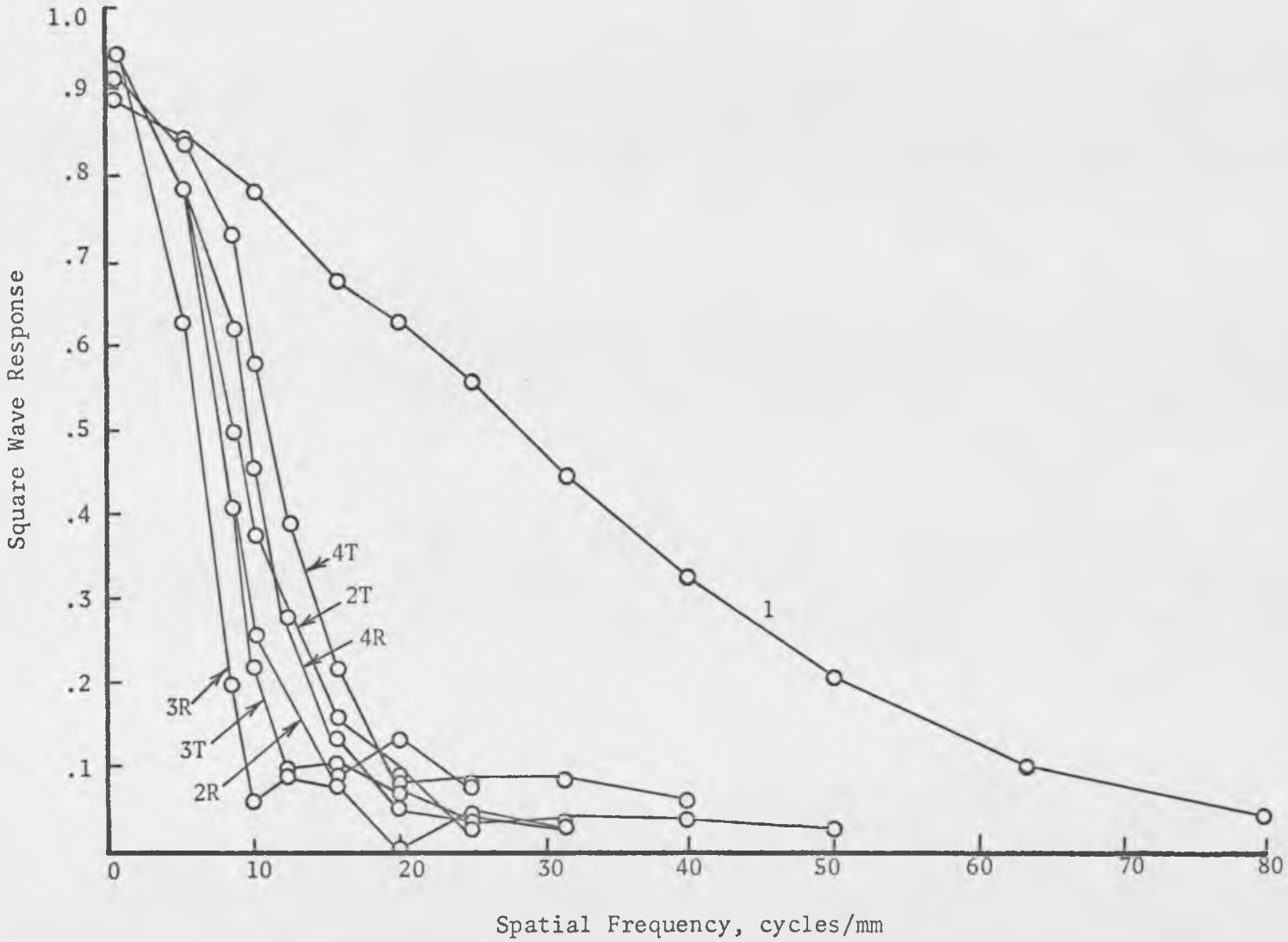

Fig. 17. Square Wave Response of the Wild Microscope (W/12/0.5; 34 mm field)

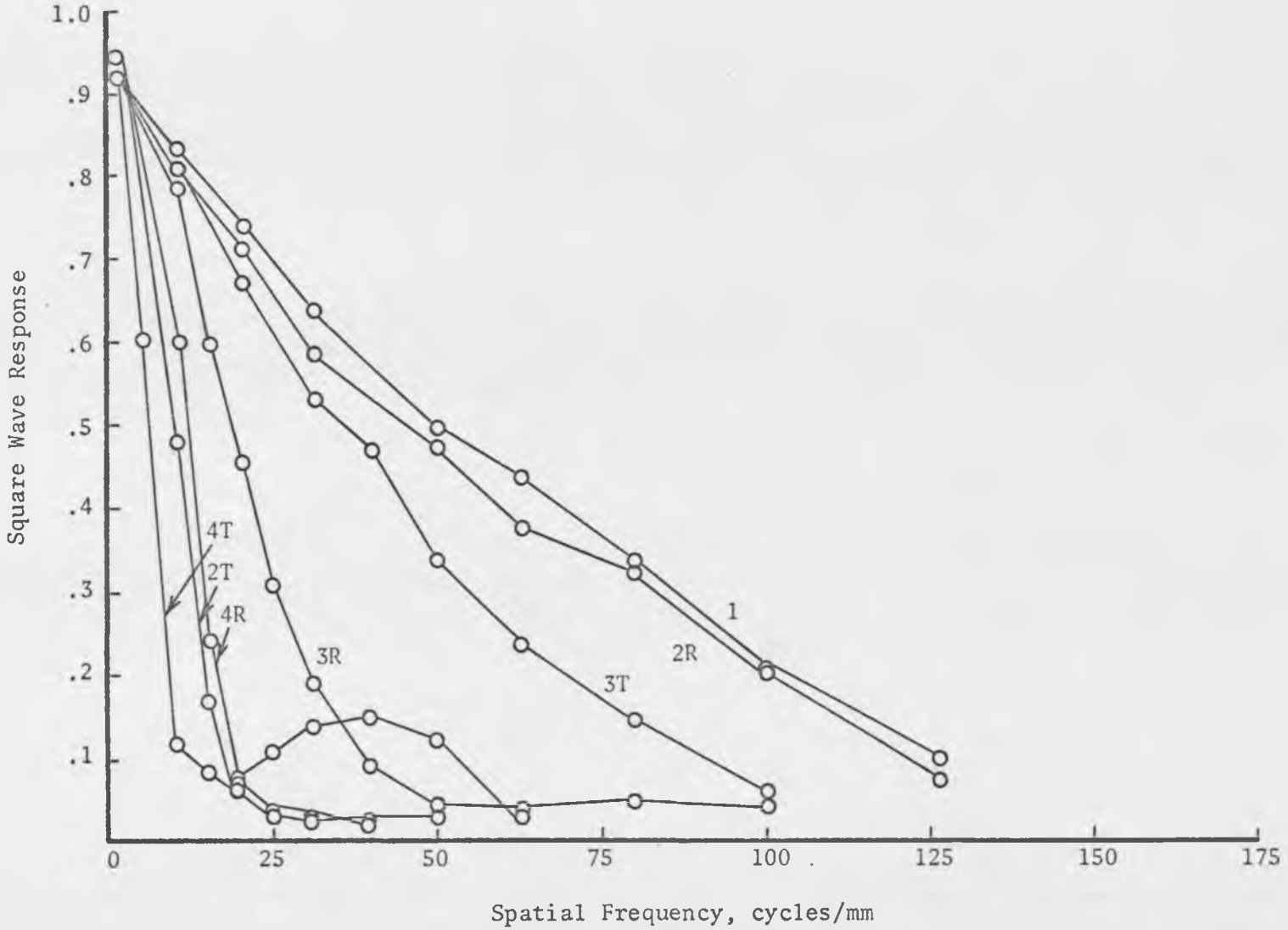

Fig. 18. Square Wave Response of the Bausch & Lomb Microscope (B/12/1; 17 mm field)

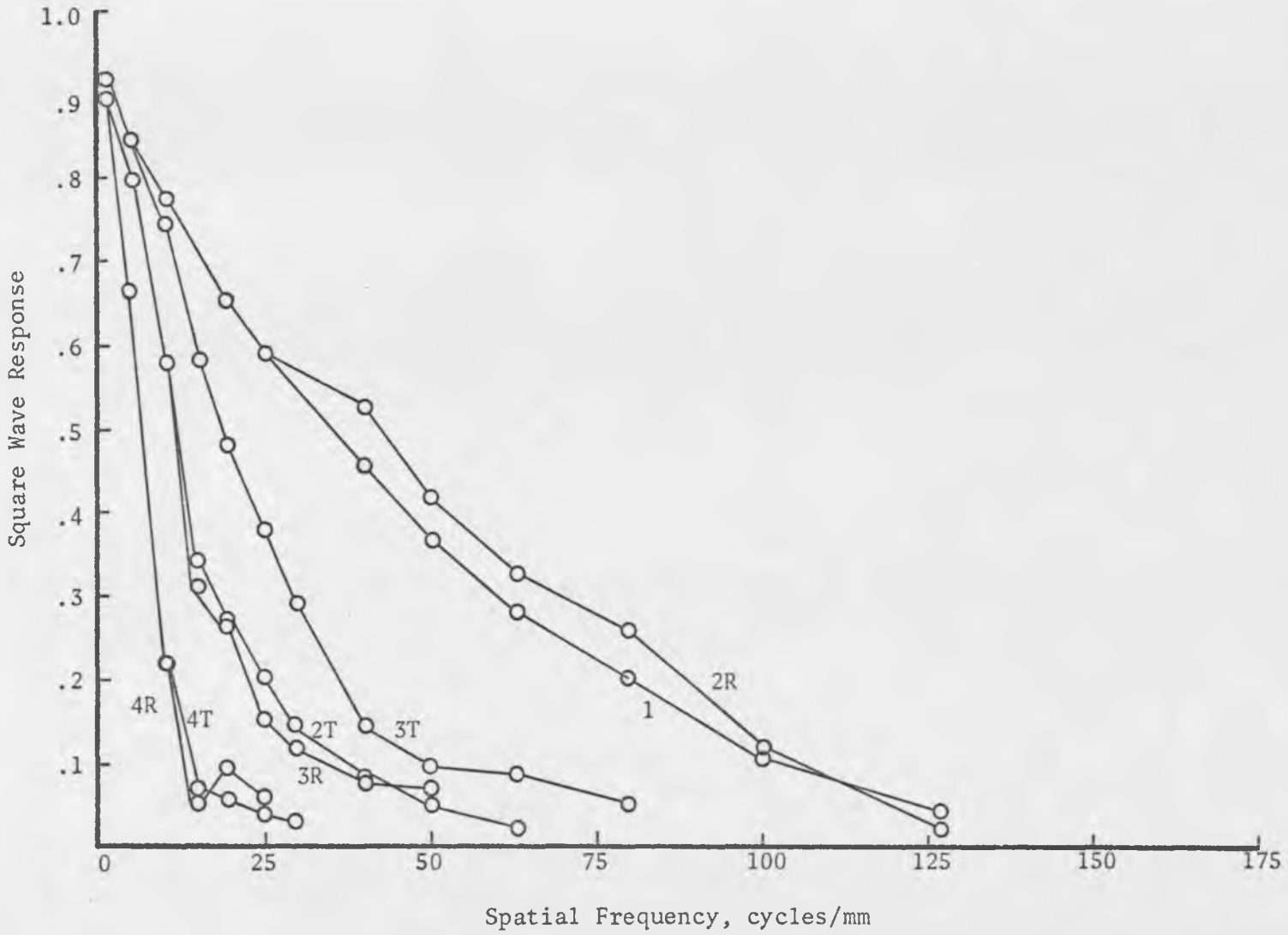

Fig. 19. Square Wave Response of the Bausch & Lomb Microscope (B/25/0.5; 17 mm field)

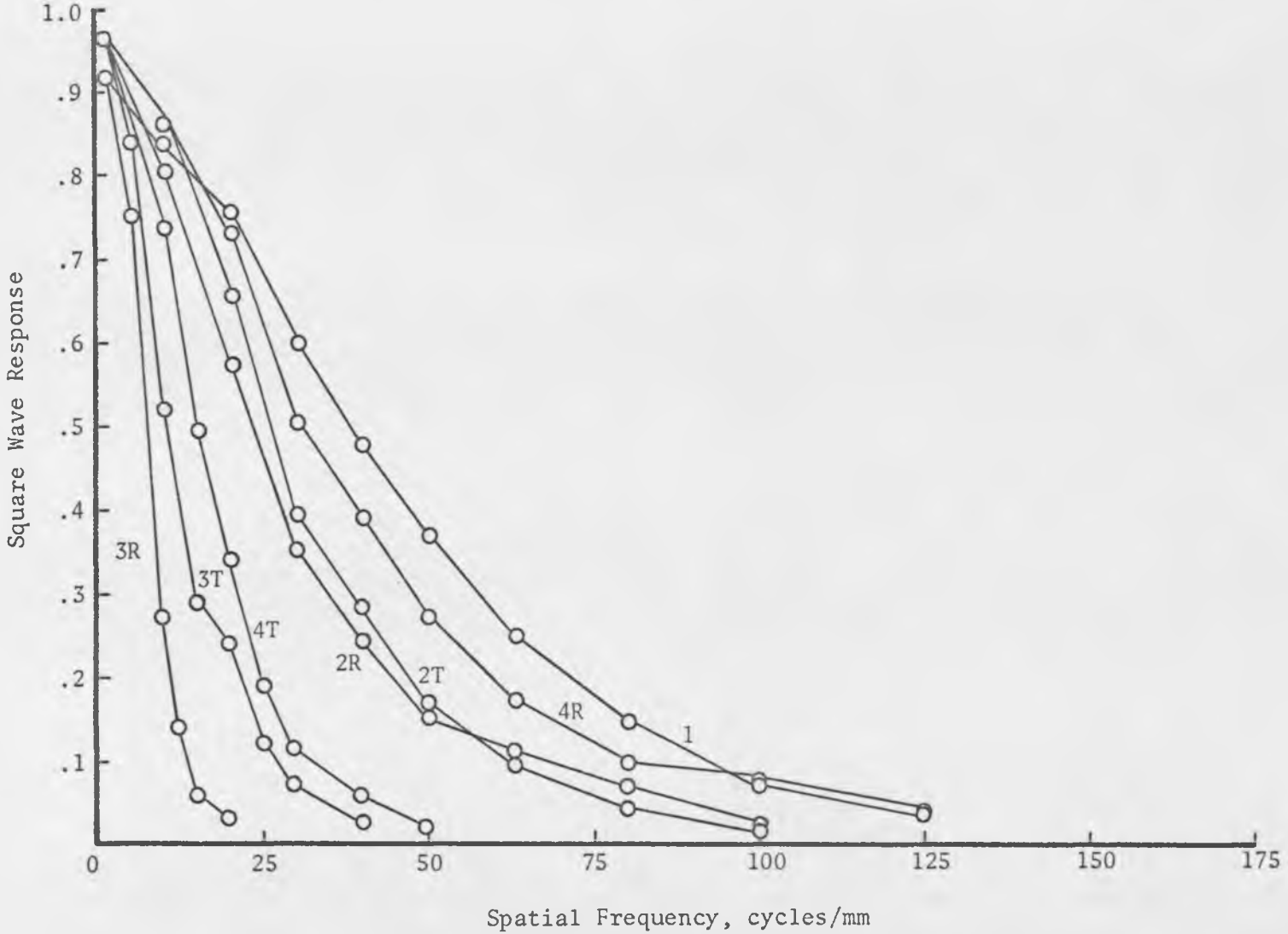

Fig. 20. Square Wave Response of the Olympus Microscope (0/13/1; 17 mm field)

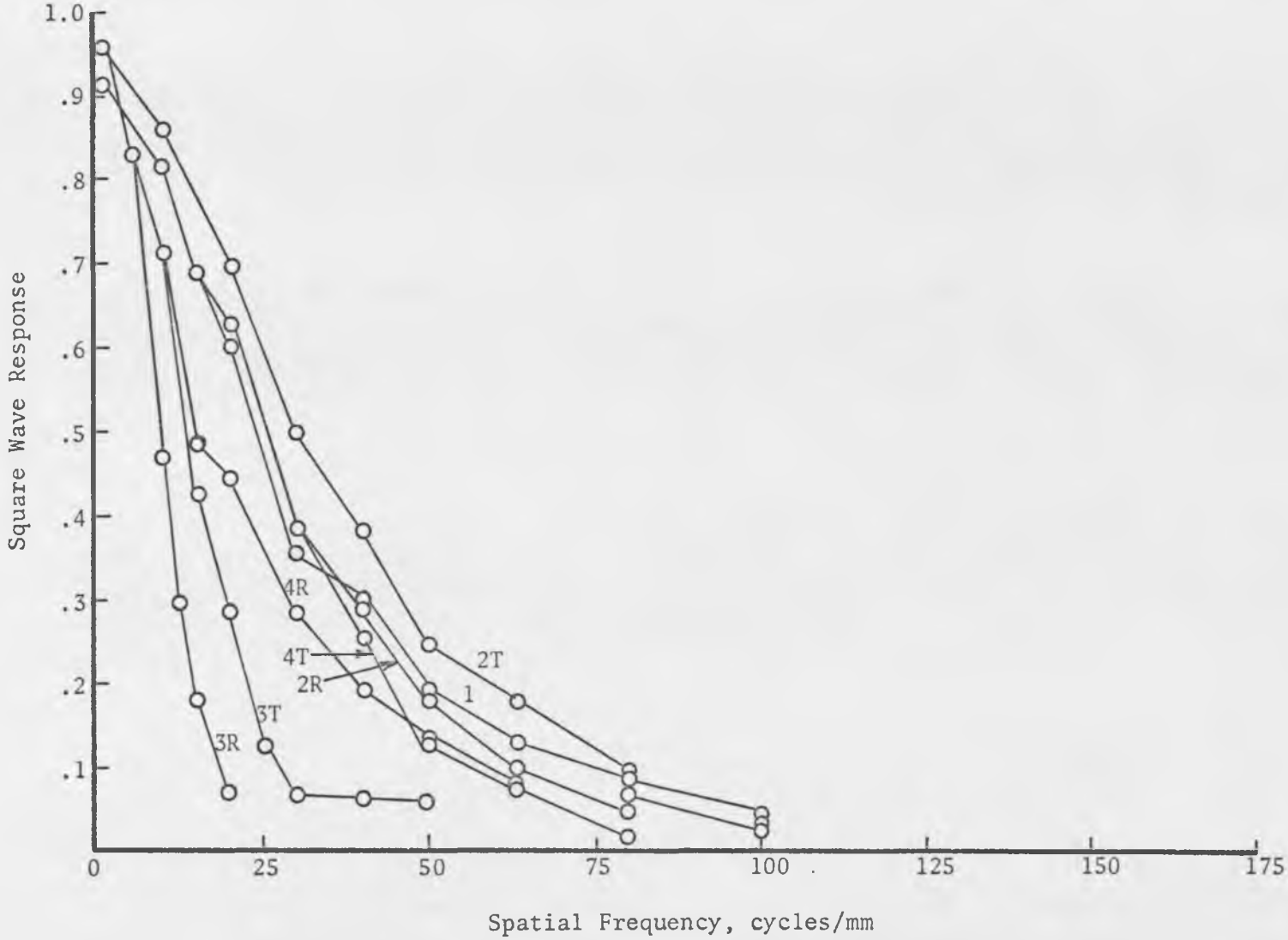

Fig. 21. Square Wave Response of the Olympus Microscope (0/27/0.5; 17 mm field)

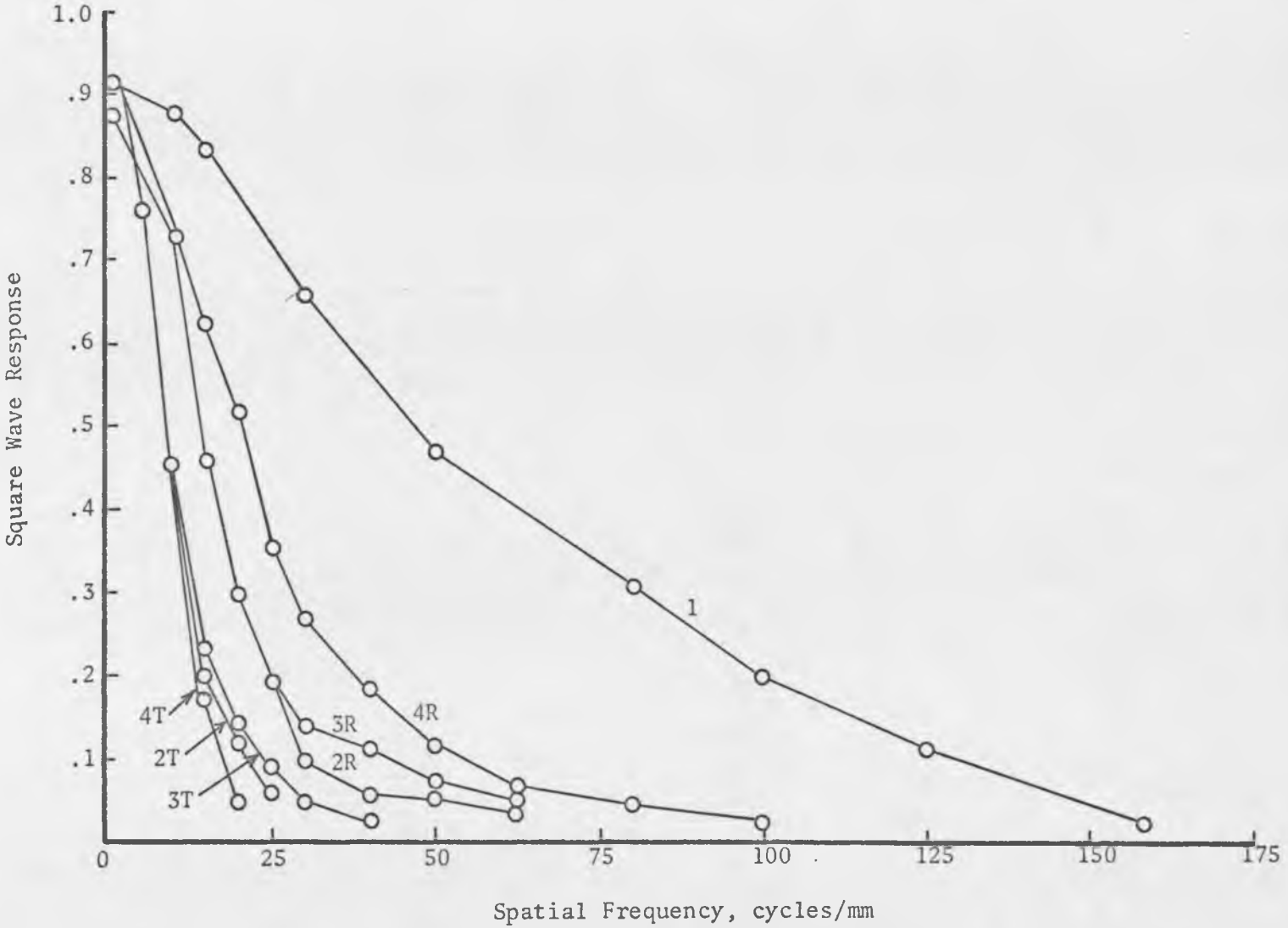

Fig. 22 Square Wave Response of the Wild Microscope (W/6/2; 17 mm field)

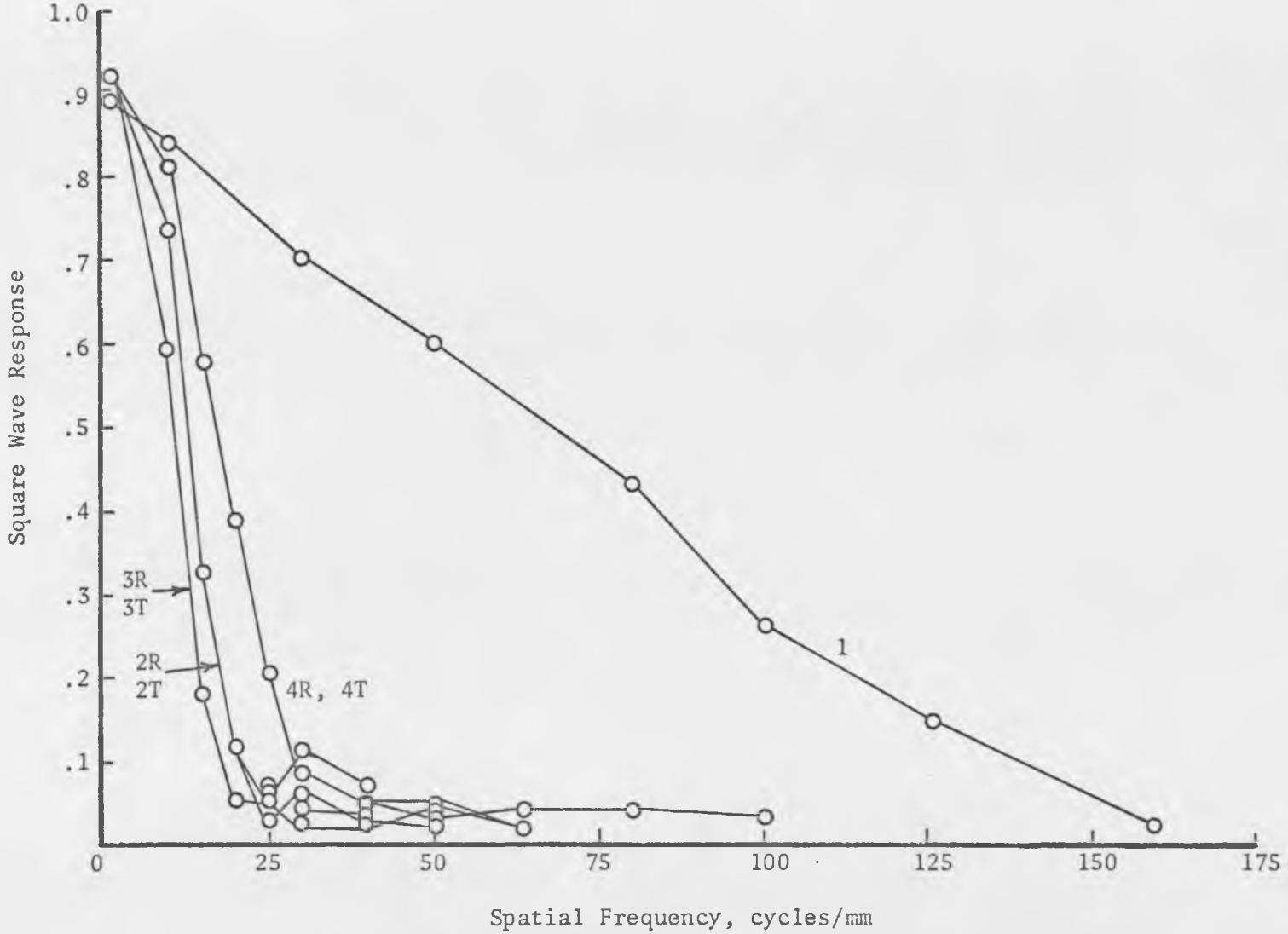

Fig. 23. Square Wave Response of the Wild Microscope (W/12/1; 17 mm field)

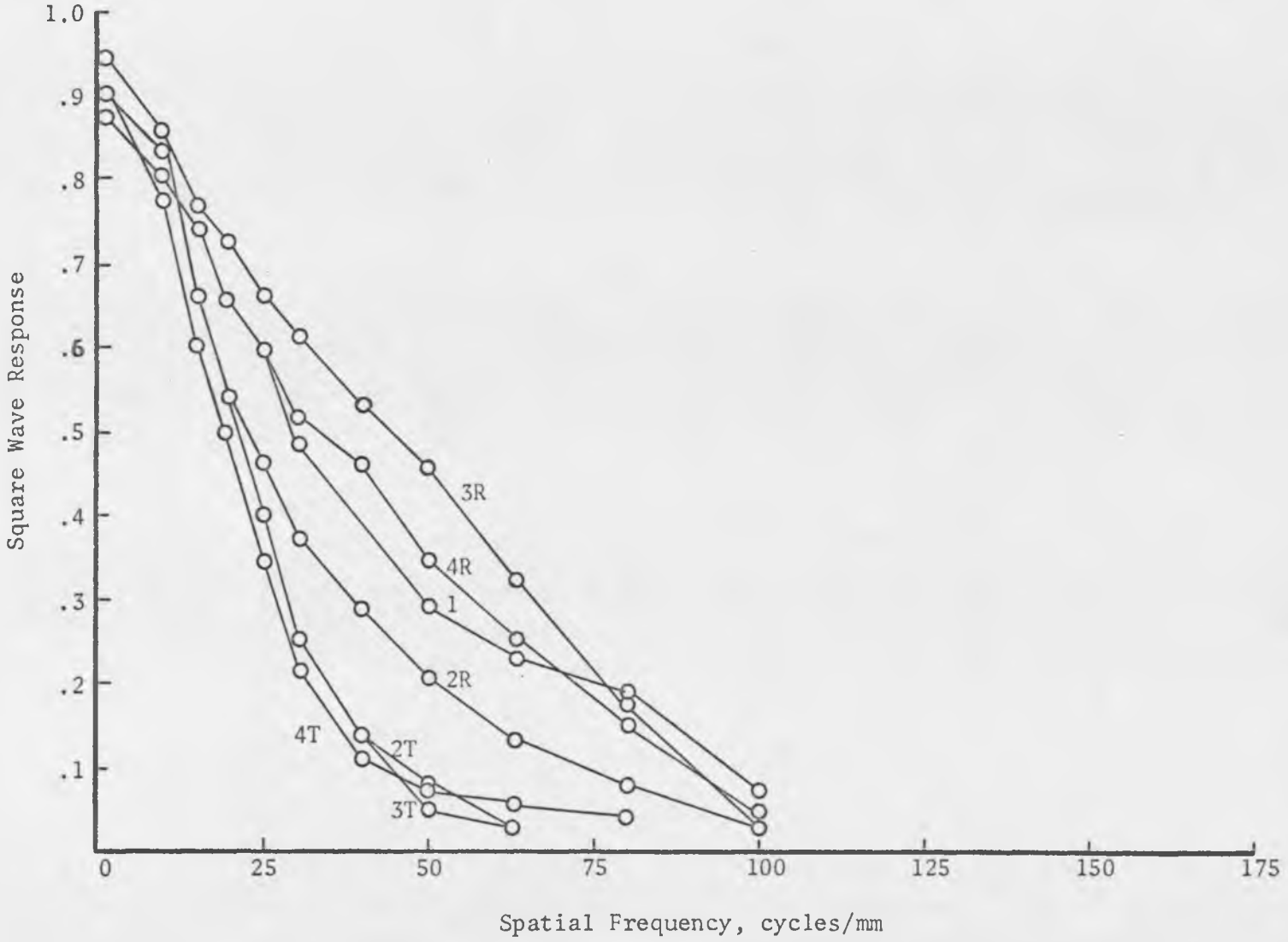

Fig. 24. Square Wave Response of the Wild Microscope (W/25/0.5; 17 mm field)

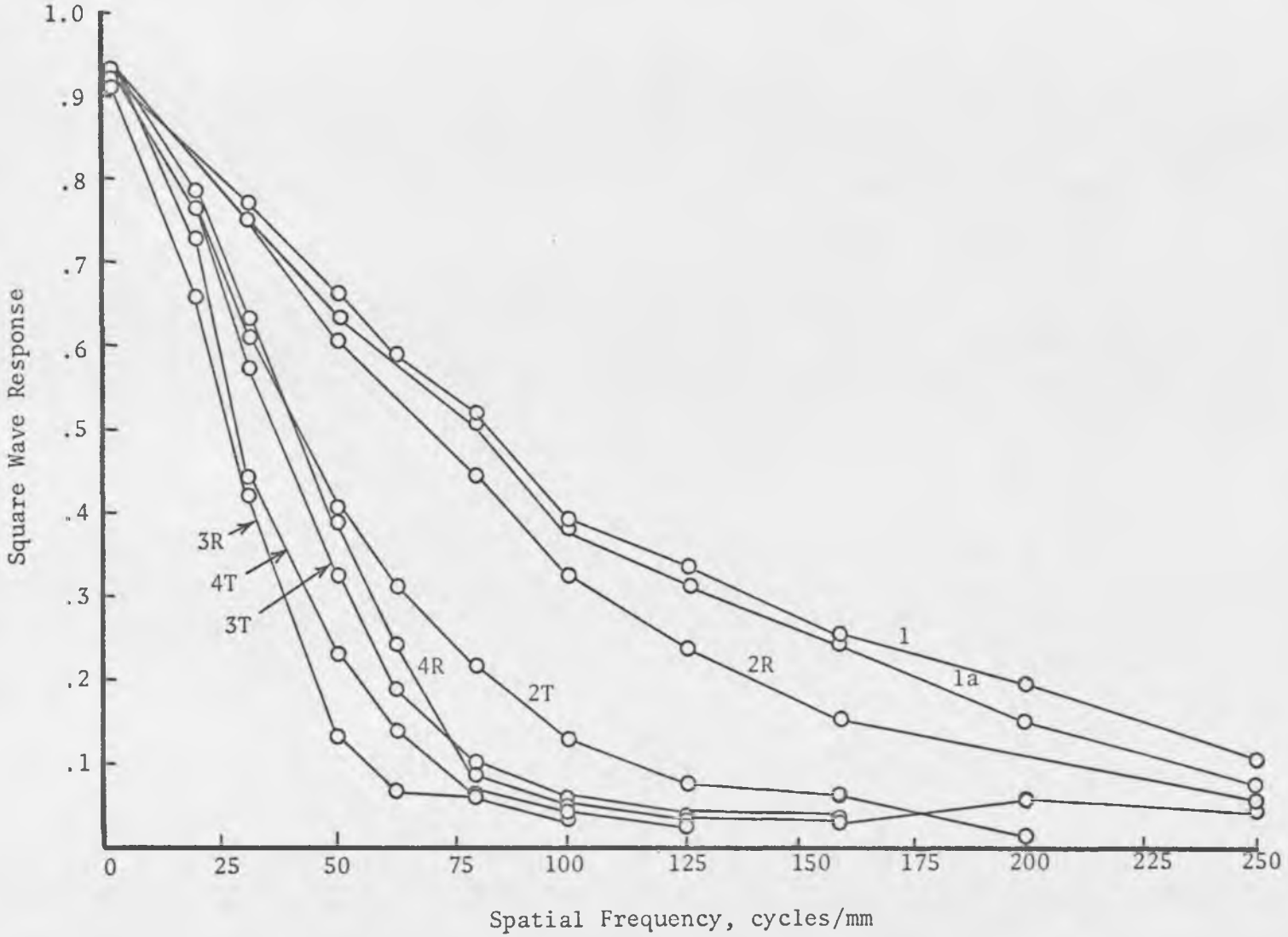

Fig. 25. Square Wave Response of the Bausch & Lomb Microscope (B/12/2; 8 mm field)

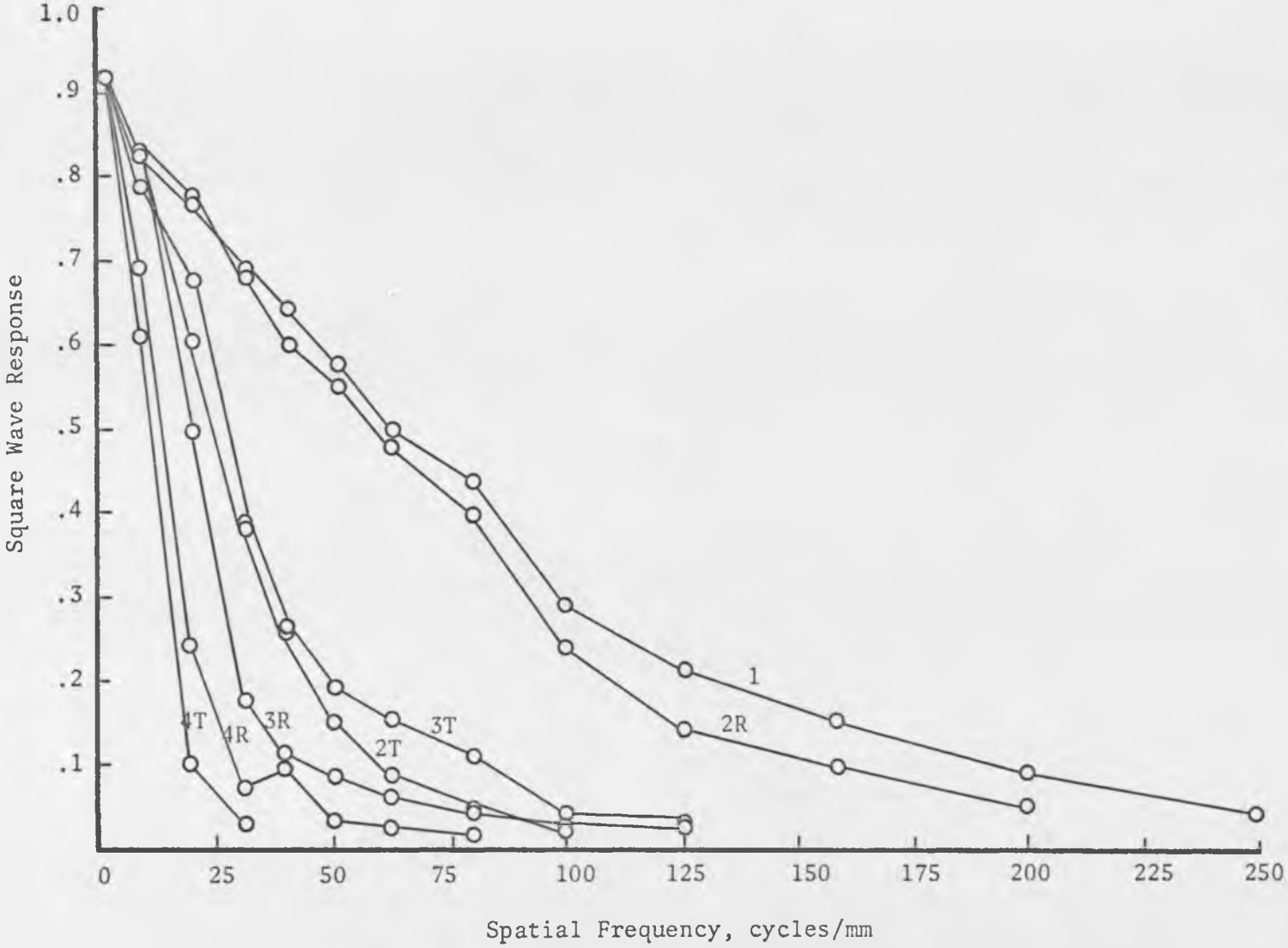

Fig. 26. Square Wave Response of the Bausch & Lomb Microscope (B/26/1; 8 mm field)

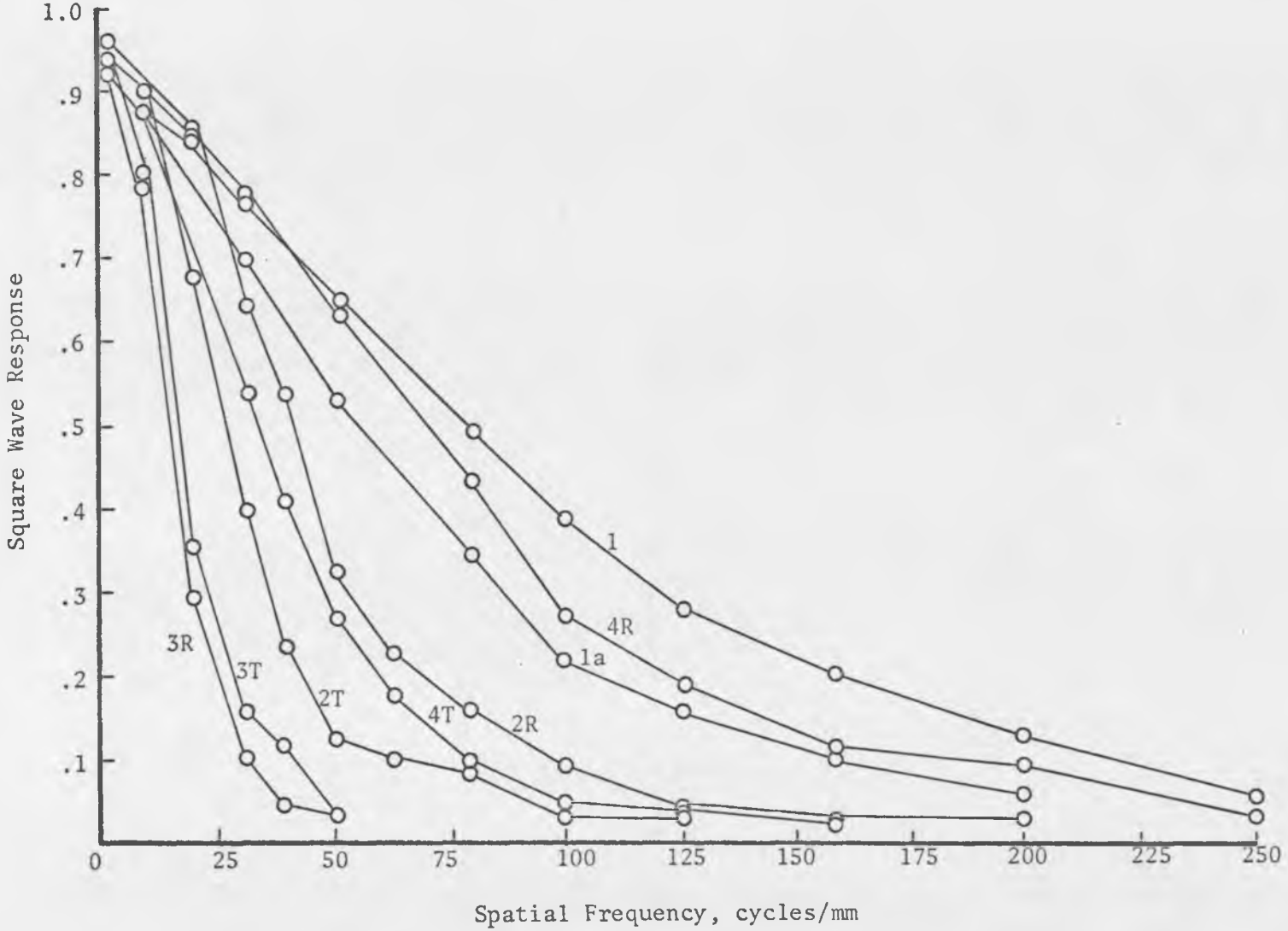

Fig. 27. Square Wave Response of the Olympus Microscope (0/13/2; 8 mm field)

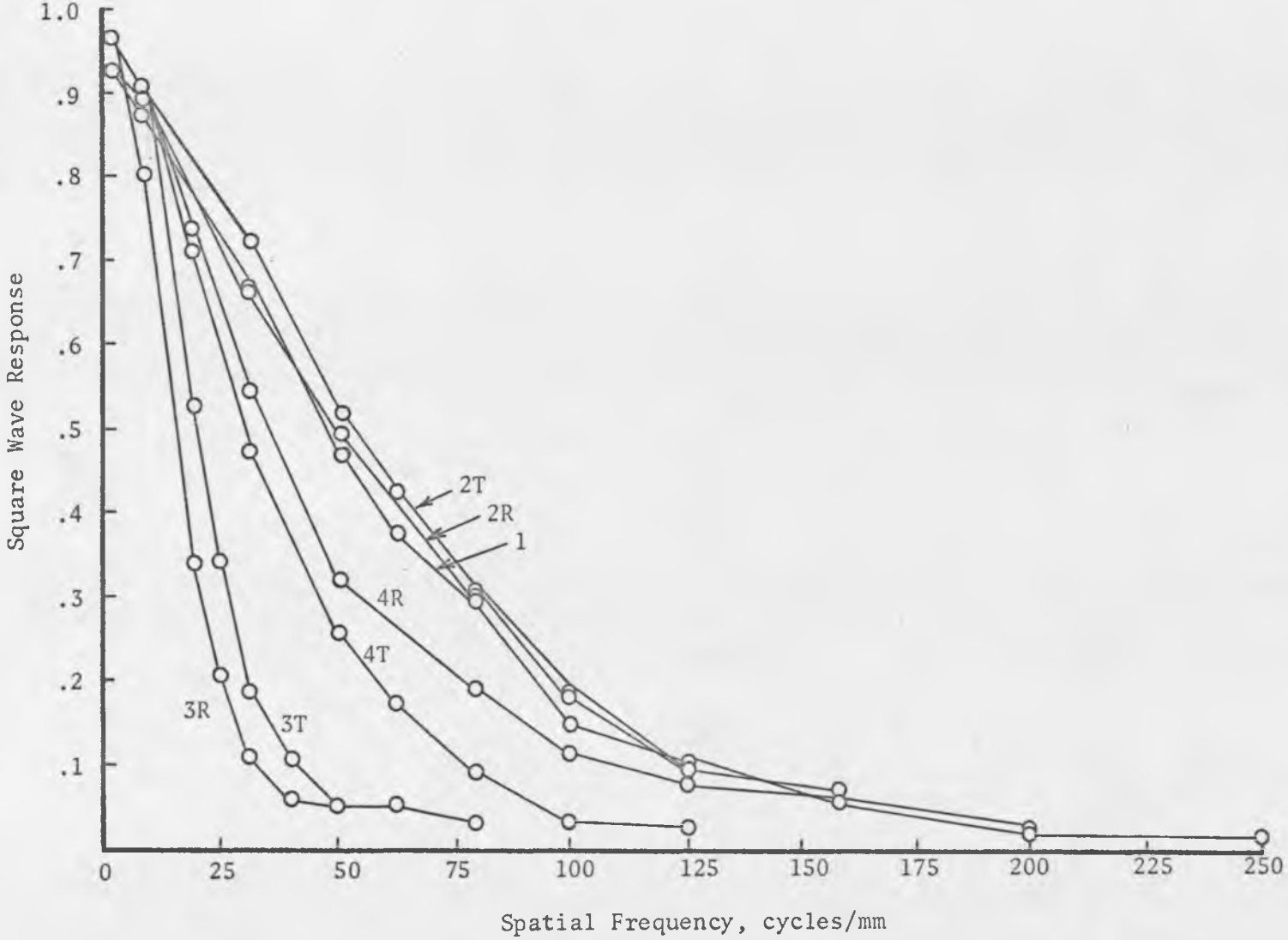

Fig. 28. Square Wave Response of the Olympus Microscope (0/27/1; 8 mm field)

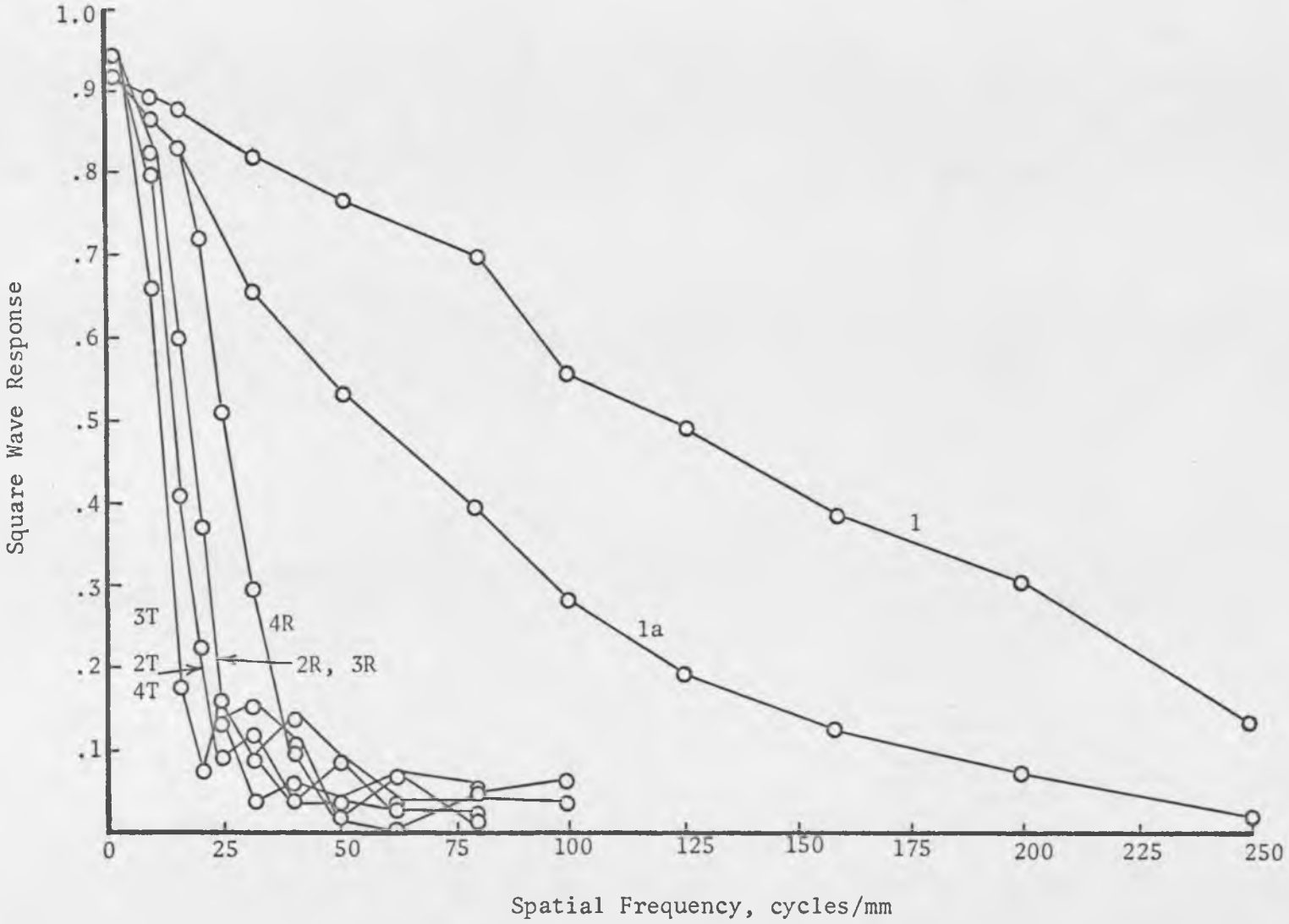

Fig. 29. Square Wave Response of the Wild Microscope (W/12/2; 8 mm field)

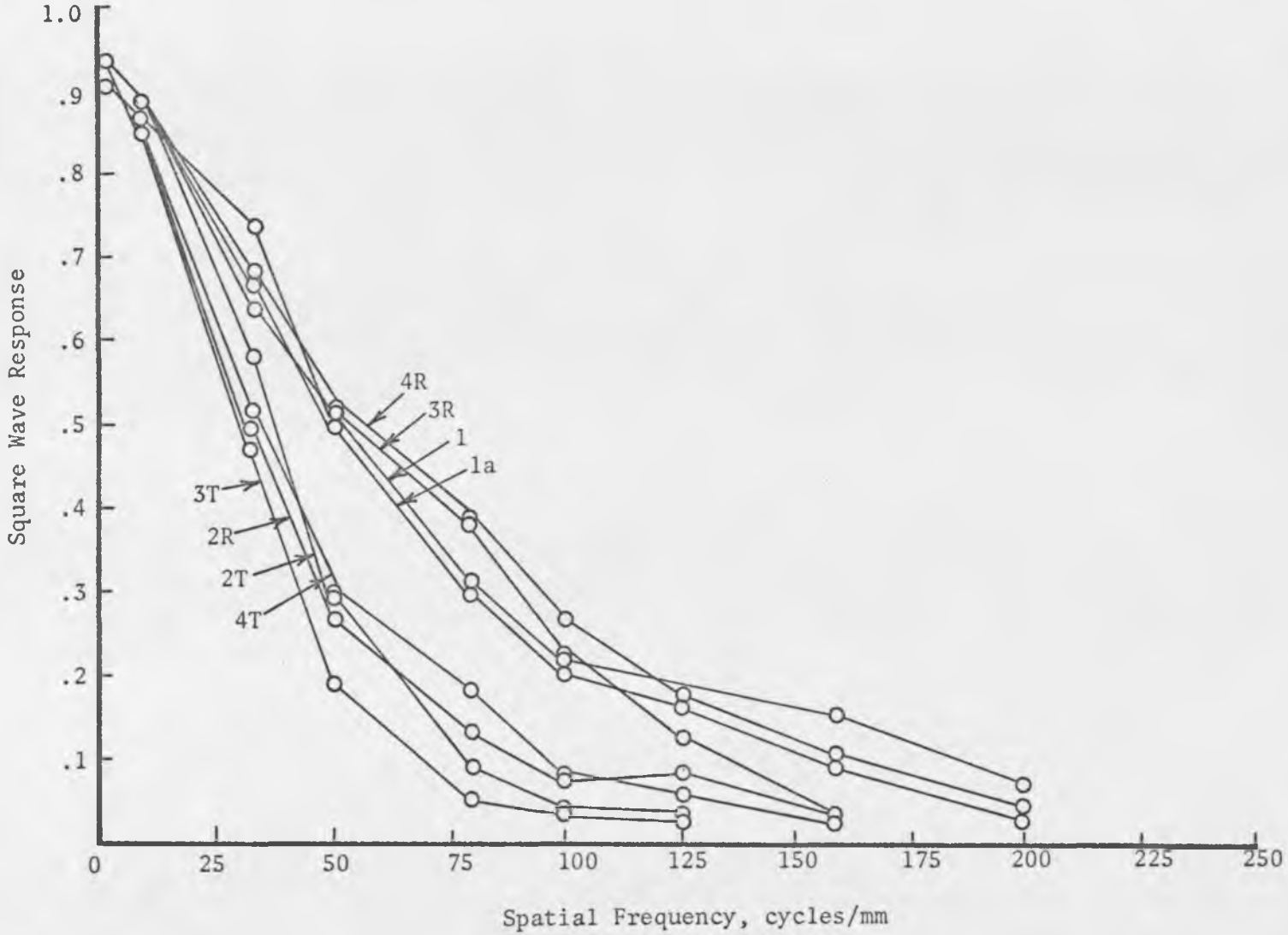

Fig. 30. Square Wave Response of the Wild Microscope (W/25/1; 8 mm field)

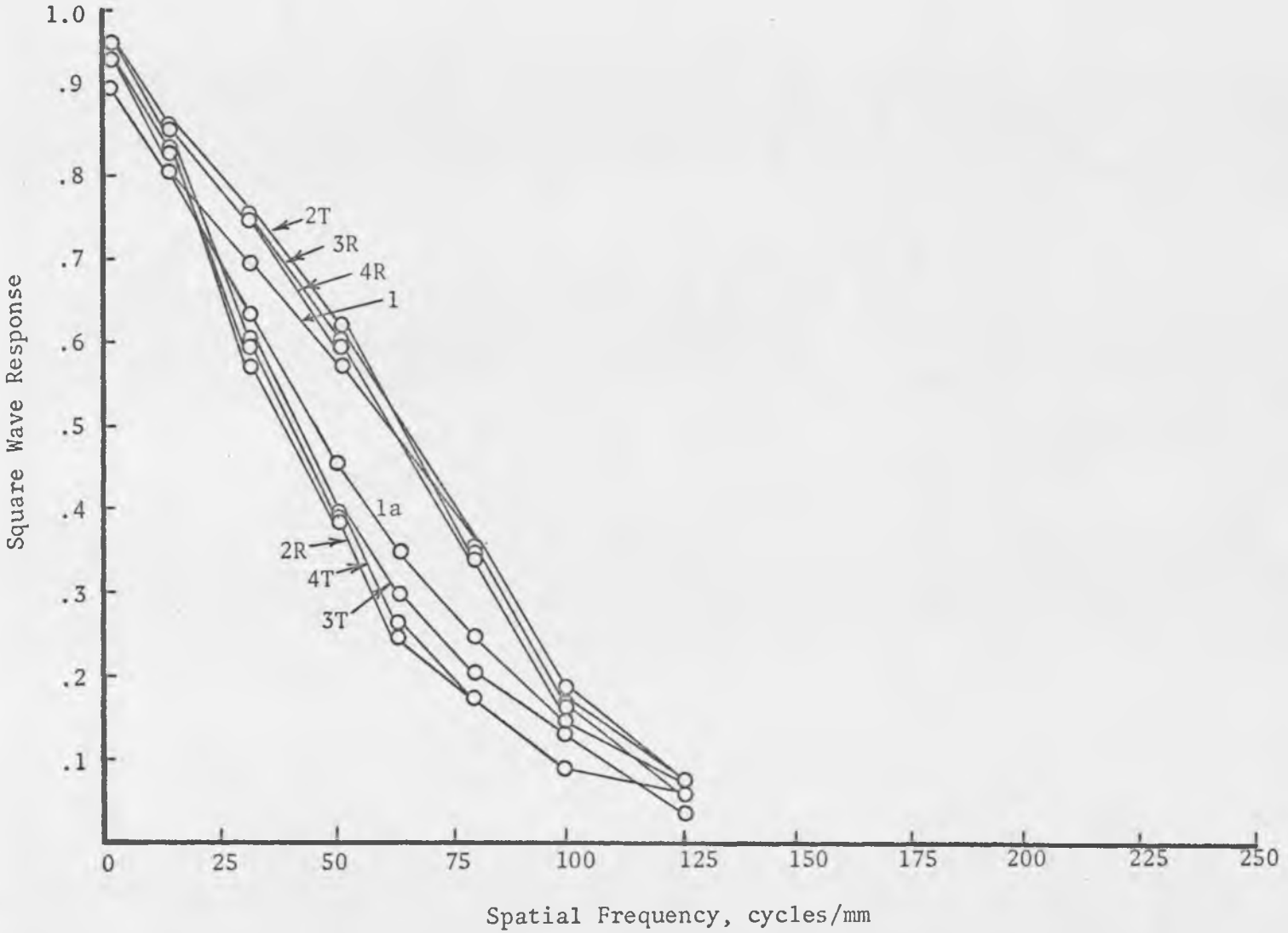

Fig. 31. Square Wave Response of the Wild Microscope (W/50/0.5; 8 mm field)

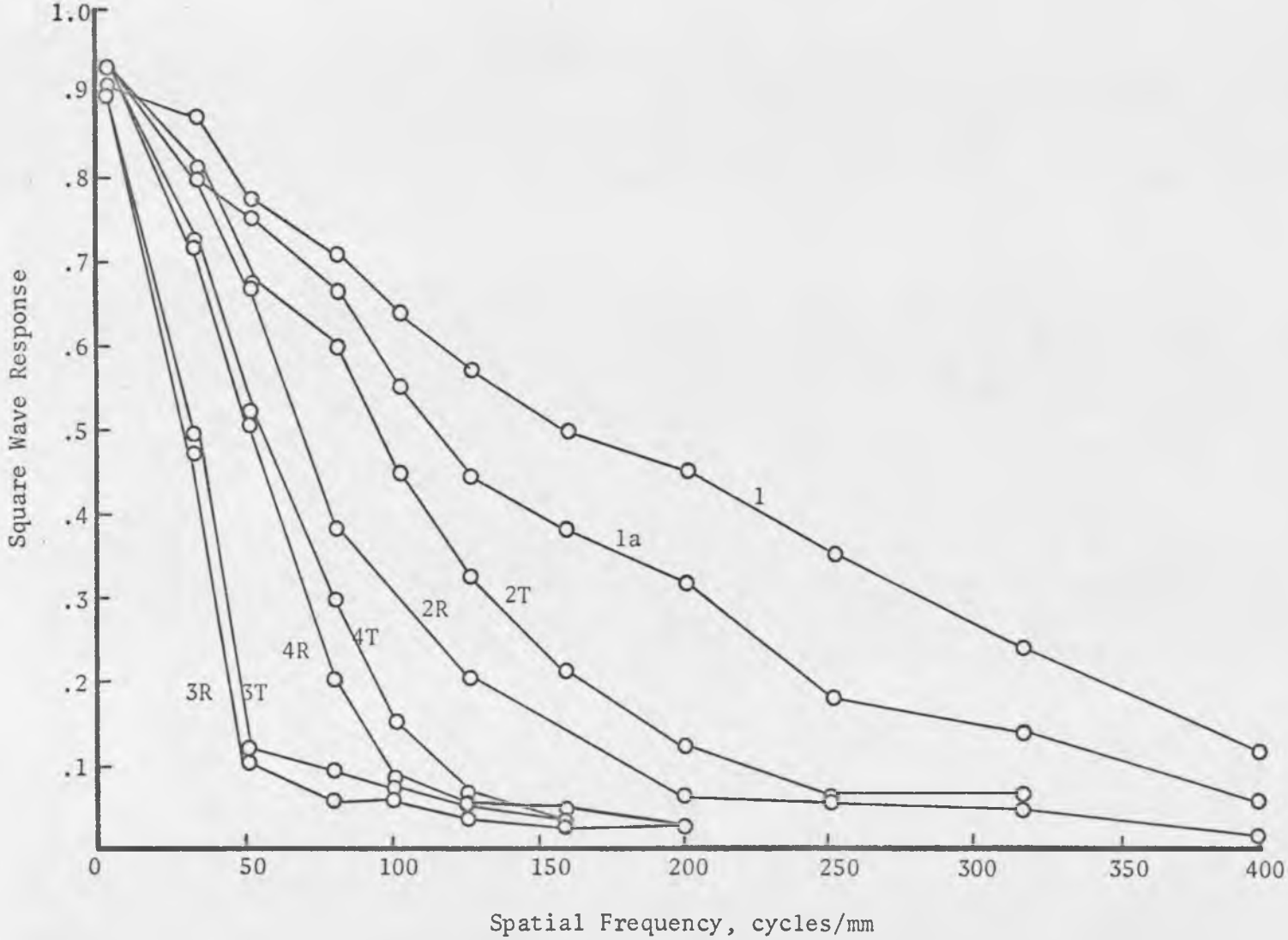

Fig. 32. Square Wave Response of the Bausch & Lomb Microscope (B/25/2; 4 mm field)

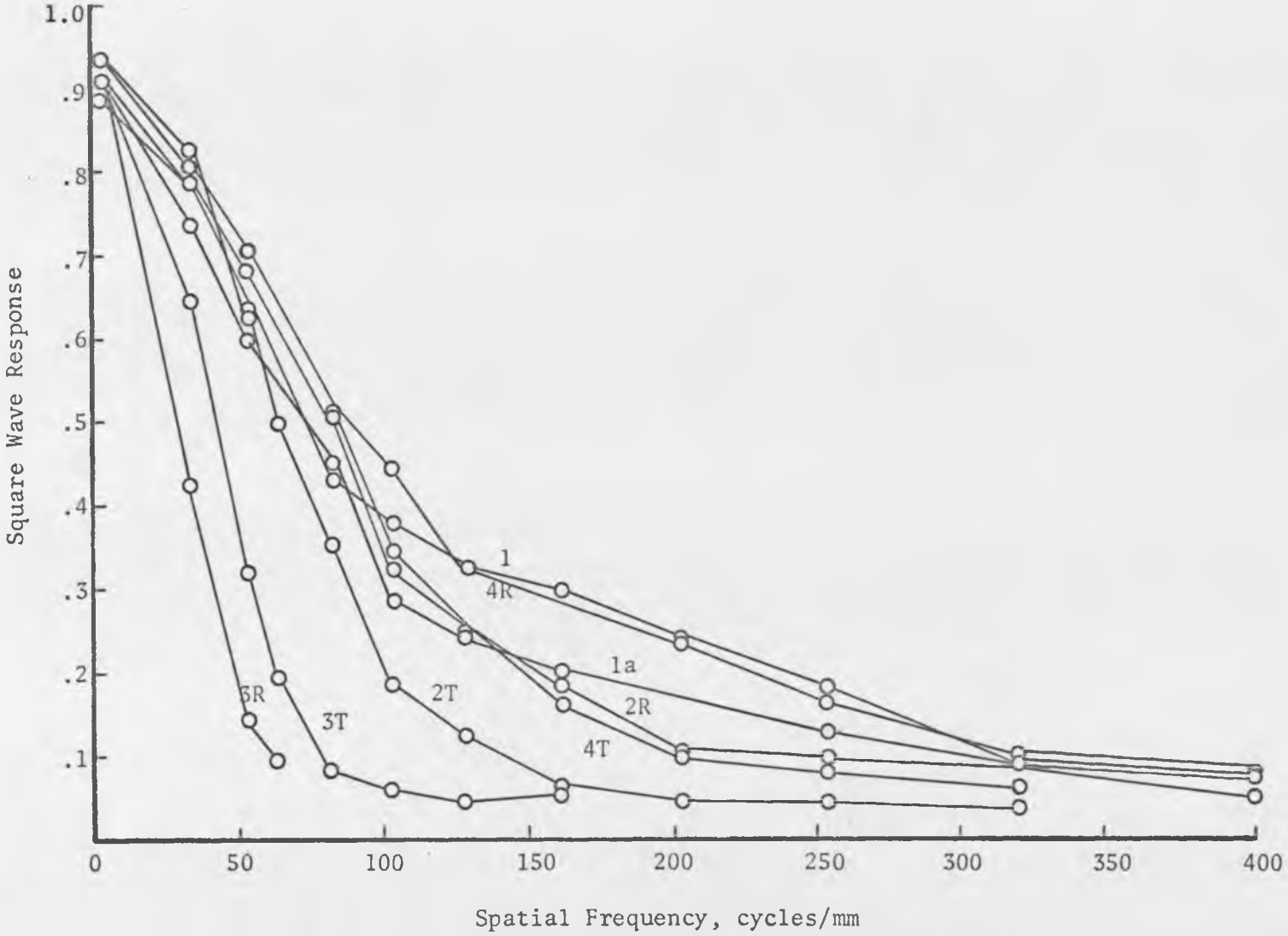

Fig. 33. Square Wave Response of the Olympus Microscope (0/27/2; 4 mm field)

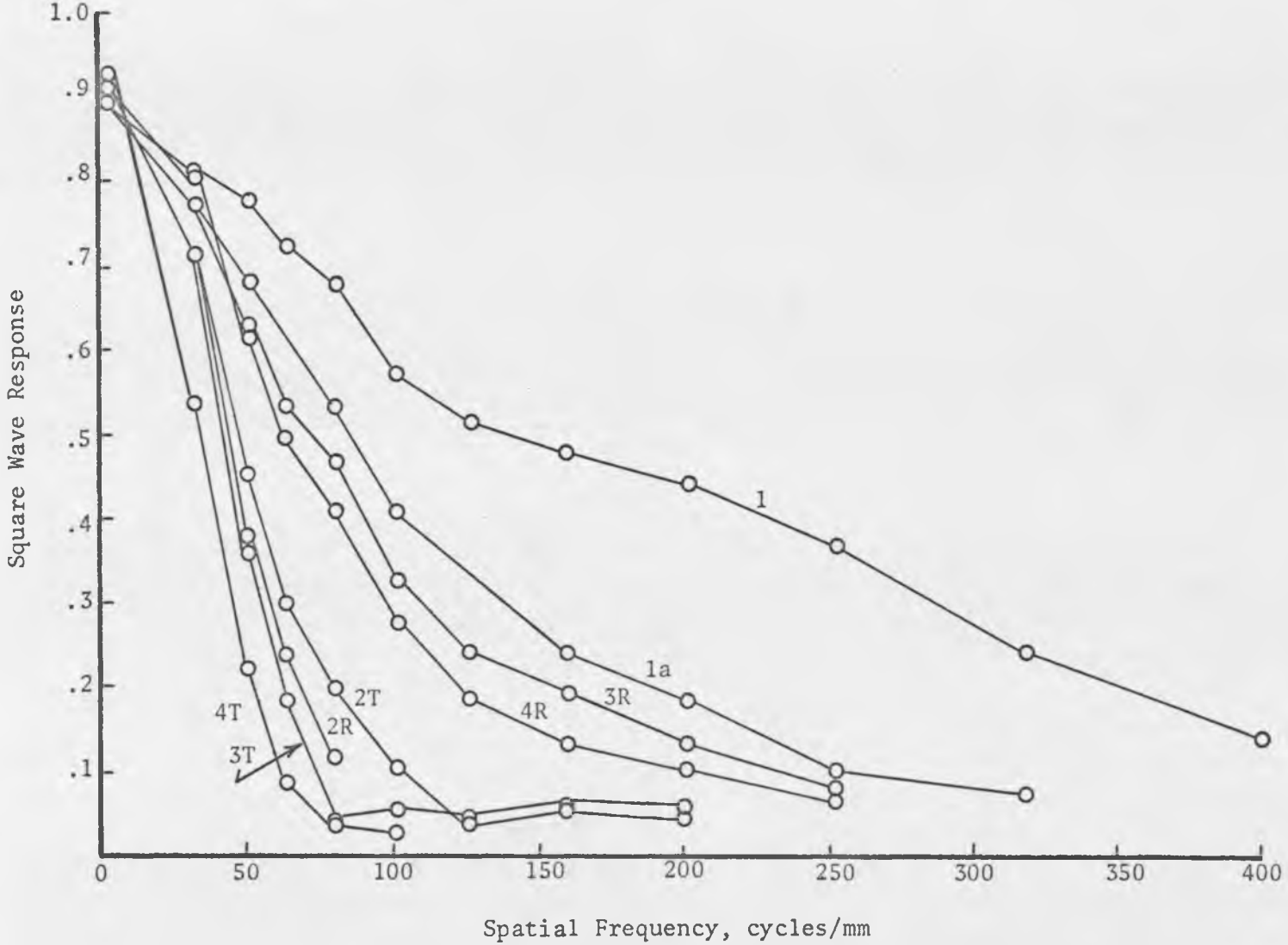

Fig. 34. Square Response Wave of the Wild Microscope (W/25/2; 4 mm field)

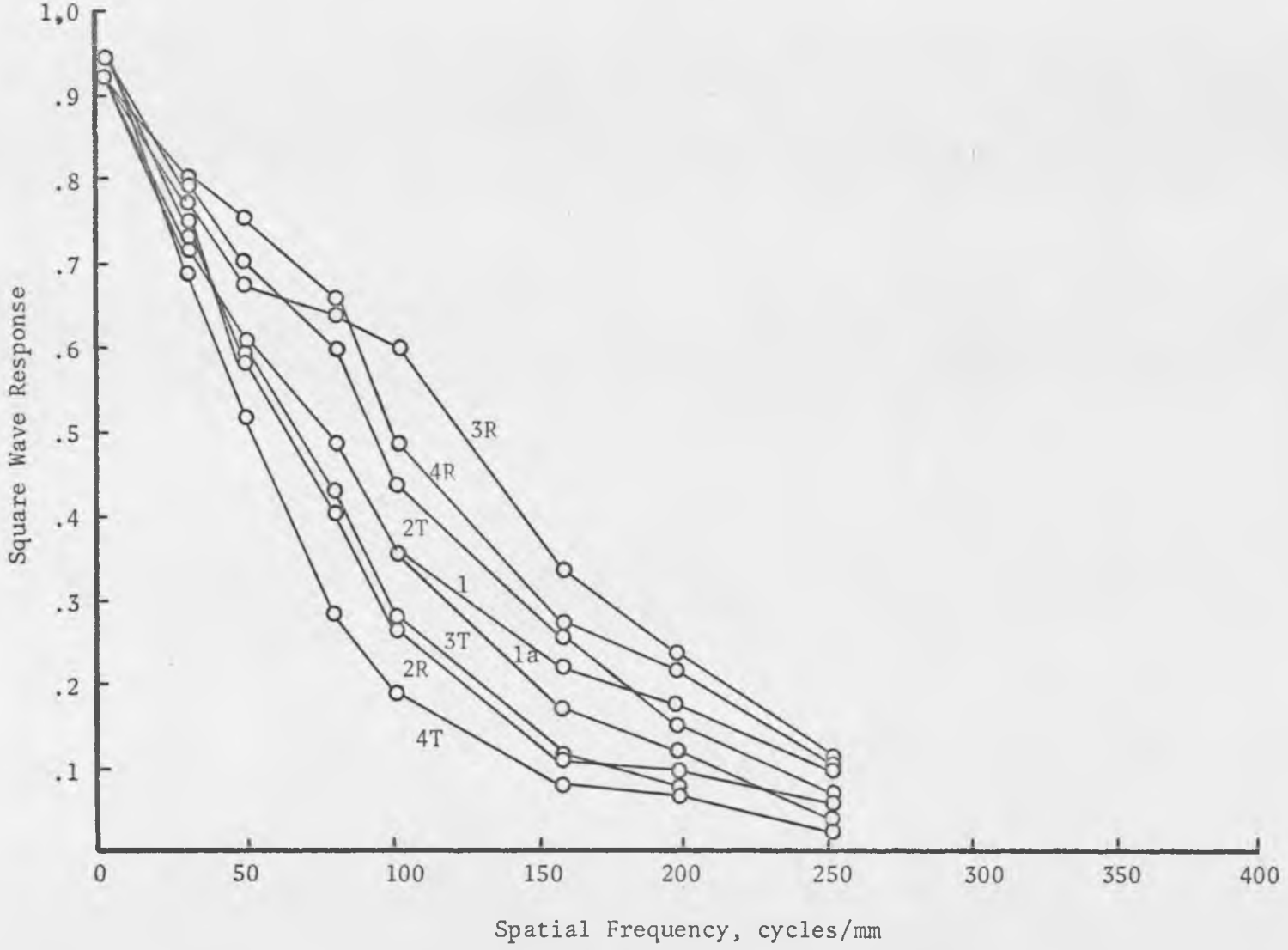

Fig. 35. Square Response Wave of the Wild Microscope (W/50/1; 4 mm field)

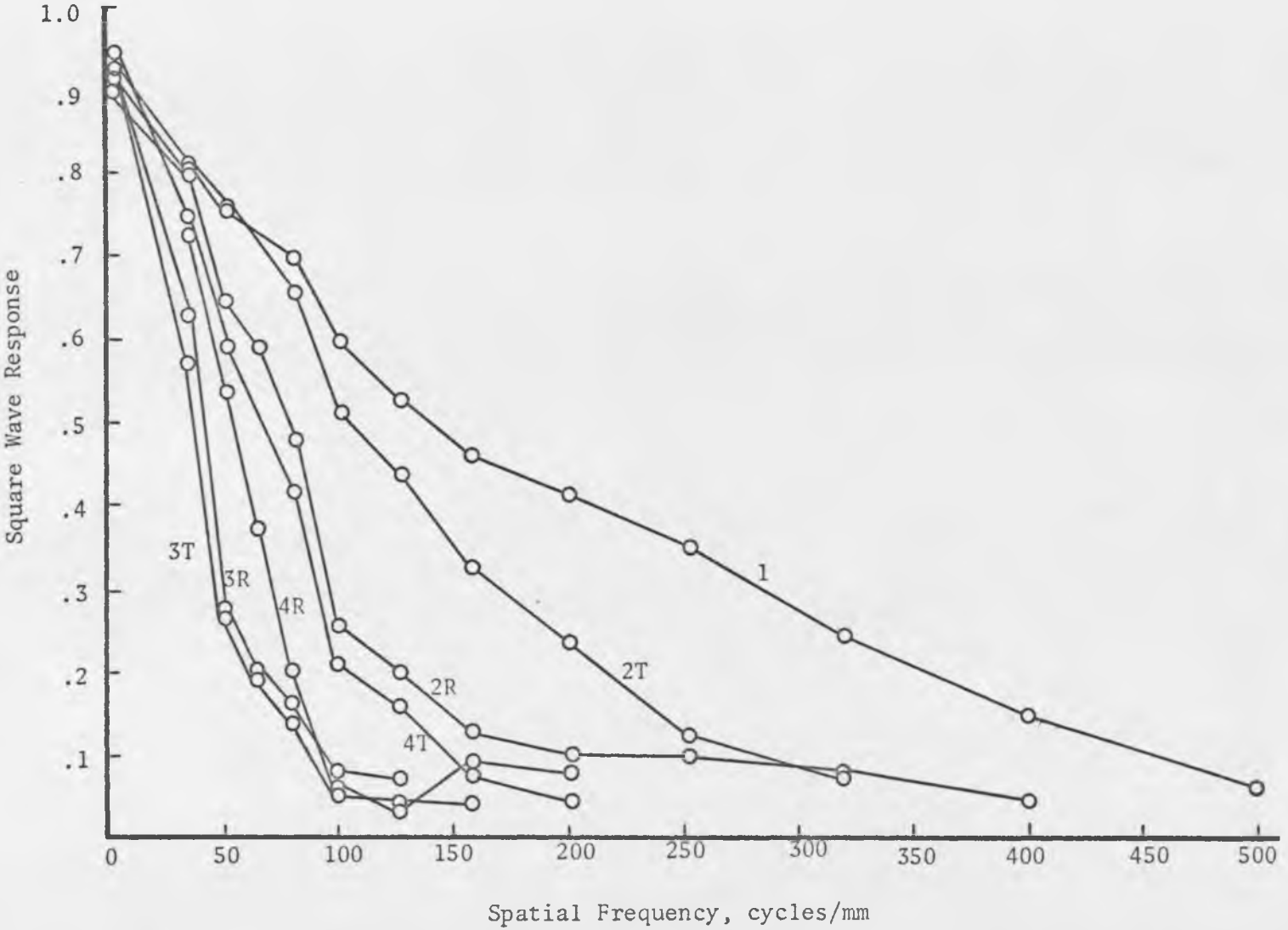

Fig. 36. Square Wave Response of the Bausch & Lomb Microscope (B/30/2; 3.3 mm field)

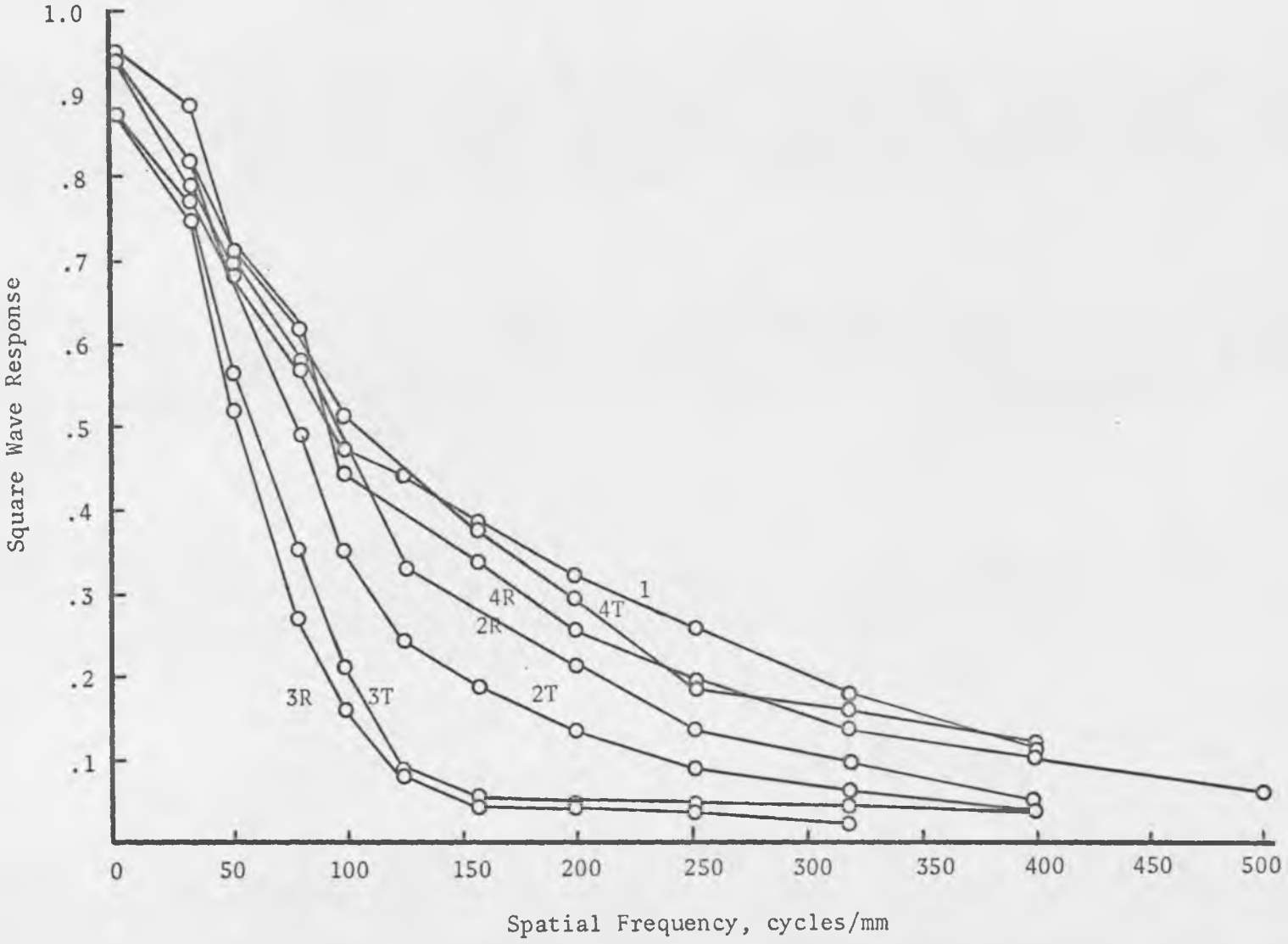

Fig. 37. Square Response Wave of the Olympus Microscope (O/40/2; 2.9 mm field)

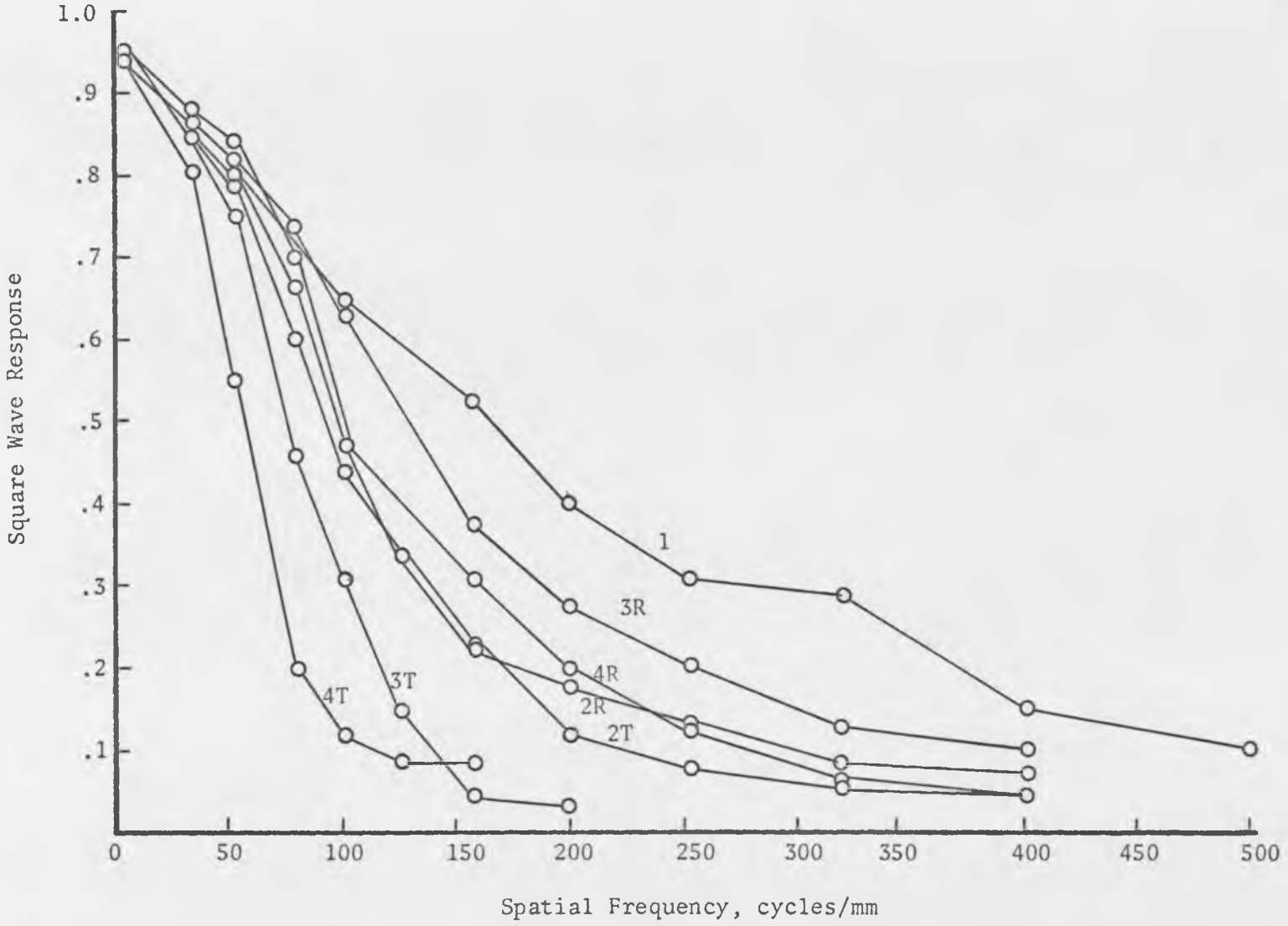

Fig. 38. Square Wave Response of the Wild Microscope (W/50/2; 2.2 mm field)

CHAPTER 6

INTERPRETATIONS

There are many ways to interpret and use SWR and SqWR information. For this study, the curves will be applied directly to two "typical" tasks encountered in photointerpretation. However, before the curves are compared, some of their general characteristics will be discussed briefly.

Some Features of the SqWR Curves

At least ten different square wave patterns were used for each SqWR curve. The frequency of the coarsest pattern was 1.25 cycles/mm, and the modulation at this frequency was generally about 0.9. The scale of the curves is such that 1.25 cycles/mm is effectively 0 cycles/mm. Since the modulation should be 1 at 0ℓ/mm, the 10 percent decrease in modulation at 1.25 cycles/mm is caused by scattered light and is predicted by Equation (7) (Chapter 3) to be given by

$$M = \frac{I_{max} - I_{min}}{I_{max} + I_{min} + 2S} \quad .$$

Substituting $I_{min} \simeq 0$ and $M = 0.9$ at 1.25 cycles/mm, we find that $S = 0.05\ I_{max}$. That is, the irradiance of the scattered light in the image is about 5 percent of the maximum irradiance in the object plane.

The SqWR data points are connected by straight lines, with no attempt at smoothing the data or curve fitting. As a result, the straight line segments do not necessarily reflect the value of the SqWR between data points, particularly when the SqWR is erratic (as when it cusps). The separation (in frequency) between data points causes the plotted SqWR curves to end before they reach zero response. The last data point plotted corresponds to the highest frequency pattern which has a modulation greater than the modulation detection threshold of the equipment (about 0.03 over most of the spatial frequency range).

Some of the SqWR curves do not decrease continuously, but increase by small amounts (up to 0.15 in modulation) near the high frequency end. In some of these cases the slope of the curve changes abruptly, rather than smoothly, at an inverted cusp-like structure (for example, see 4R of B/12/0.5).

The tip of the cusp is usually plotted at a non-zero modulation because of the limited number of data points; however, it actually is located at zero modulation and indicates the frequency where the phase portion of the OTF changes sign. Some authors consider the phase reversal as a transition to negative modulus. However, we have defined the modulation as a positive quantity, and thus the SqWR must remain positive. Hence we get a cusp. The following SqWR curves have cusps, or at least have an increasing SqWR, over part of their spatial frequency range: 2R, 2T and 3T of W/12.5/1; 4R of B/12/1, B/25/0.5, B/26/1 and B/12/0.5; 3R of W/12/0.5; and all off-axis curves of W/12/2.

The repeatibility of the SqWR data appears to be quite good. Two measurements of the maximum and minimum irradiances of a test pattern will yield modulations that differ by no more than approximately 0.03. This assumes that the test target is not moved relative to the microscope between measurements. The major portion of the difference arises from calculating the modulation (see Chapter 4).

The suitability of using the measured SqWR curves as bases for comparing the microscopes depends on whether or not these particular curves are representative of the microscopes. There are four main factors, whose effects are unfortunately not fully known, which could influence the worth of the measured SqWR curves. First, only one microscope from each manufacturer was tested, and we do not know if it is typical of all microscopes of that type. Second, only three off-axis field positions and two test target orientations were included in the measurements. Variations in SqWR across the field could be such that the three points where measurements were made do not even closely represent an "average" off-axis field positon. Third, the SqWR was measured at only one focal position, that giving maximum on-axis resolution, and the SqWR is not necessarily optimum at this position. Fourth, the off-axis SqWR was measured in the same focal plane as the on-axis SqWR. However, the eye, unlike the detection stage, can accommodate and effectively improve the off-axis response if the degradation is due to focus errors. Therefore, the measured off-axis curves represent a "worst case", such as would be seen with an eye having little or no accommodation.

Comparing the Microscopes for Two Photointerpretation Tasks

The SqWR curves will now be compared to determine which microscope and which lens combinations are most suitable for performing "typical" photointerpretation tasks. The two tasks we will consider are: (1) scanning imagery as if searching for a target, and (2) examining the target in detail. Of course, these are not the only tasks for which the microscopes can be evaluated; other tasks, with different requirements, can be treated in a similar manner. However, the tasks we will use are fundamental to photointerpretation, and are representative of how microscopes are used by photointerpreters.

When a target is examined in detail, usually it is positioned in the center of the microscope field since on-axis performance is assumed to be better than off-axis performance, and since the photointerpreter can better relate the target to its surroundings in this position. For some of the measured SqWR curves, the on-axis SqWR is inferior to the off-axis SqWR for a particular orientation of the test target; however, the SqWR for the other orientation is inferior to the on-axis SqWR (for example, W/25/0.5 and B/25/0.5). Only for E/27/1 and E/27/0.5 do both orientations of an off-axis position (2) have a better SqWR than on-axis. Nevertheless, for the detailed examination task we assume that the target is on-axis, and that only the on-axis SqWR is important; the off-axis SqWR is of little or no concern.

The on-axis SqWR curves are shown in Figures 39-43 for the 34 mm, 17 mm, 8 mm, 4 mm and minimum field sizes, respectively. For

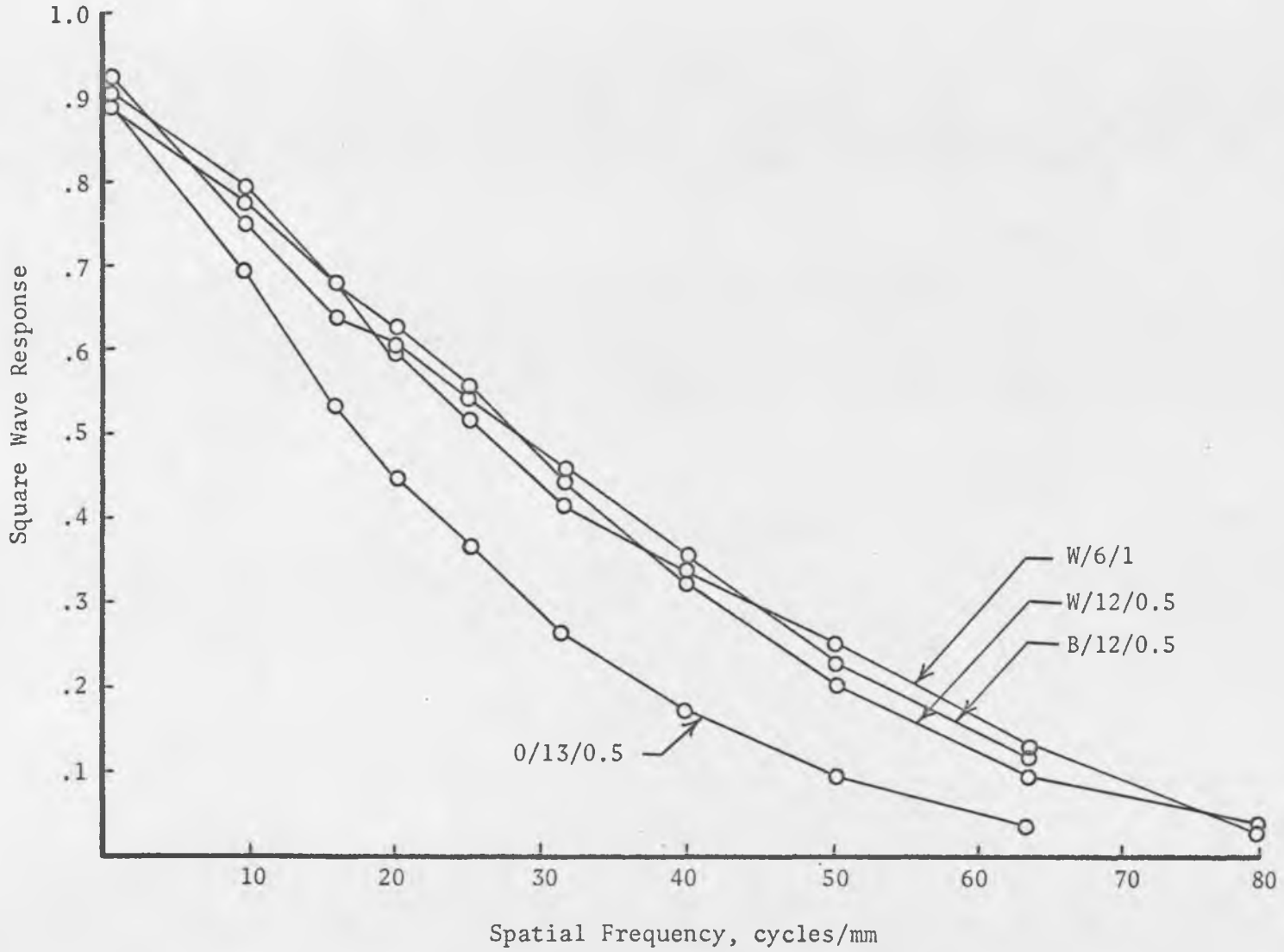

Fig. 39. On-Axis SqWR for a 34 mm Field

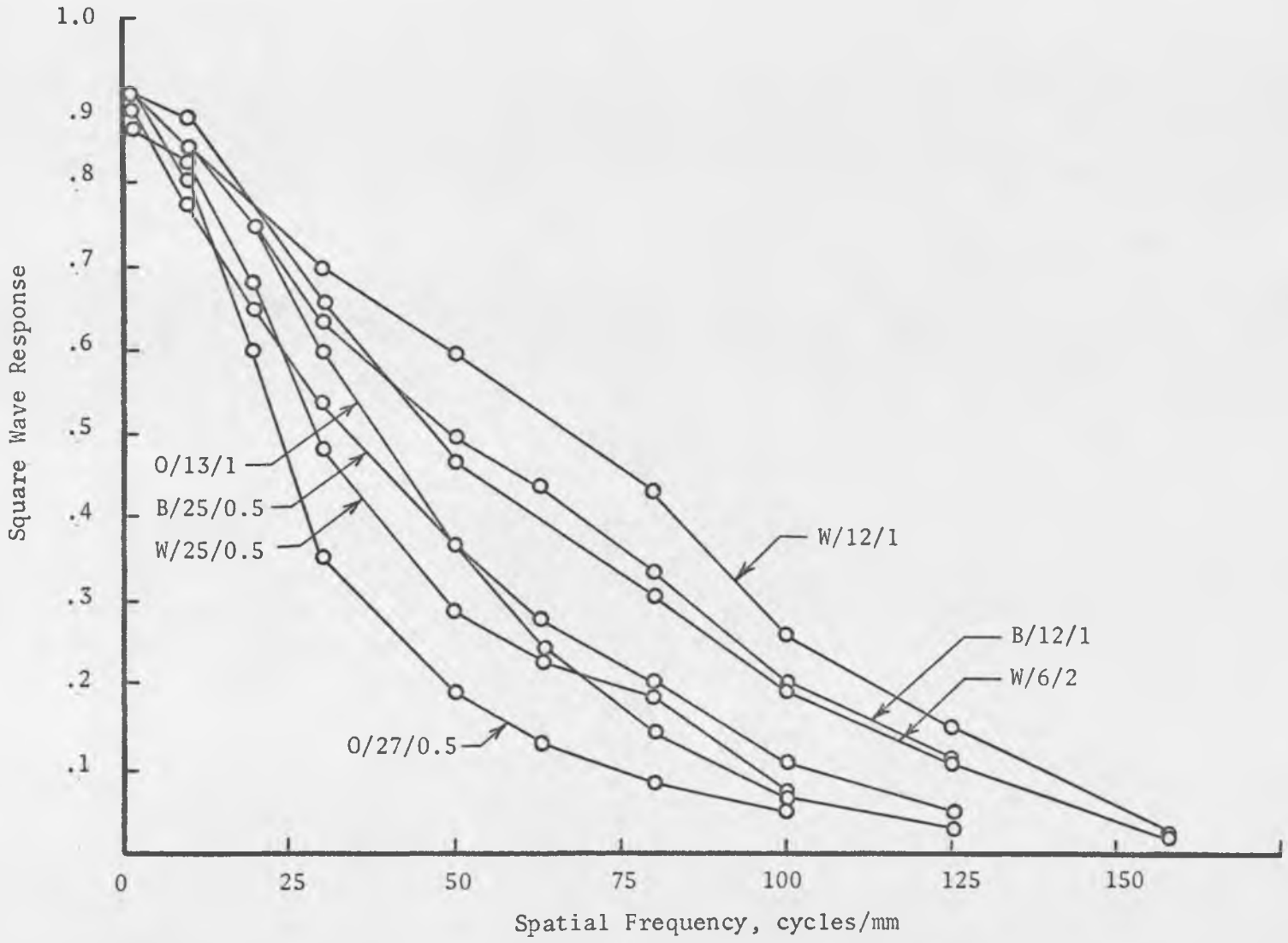

Fig. 40. On-Axis SqWR for a 17 mm Field

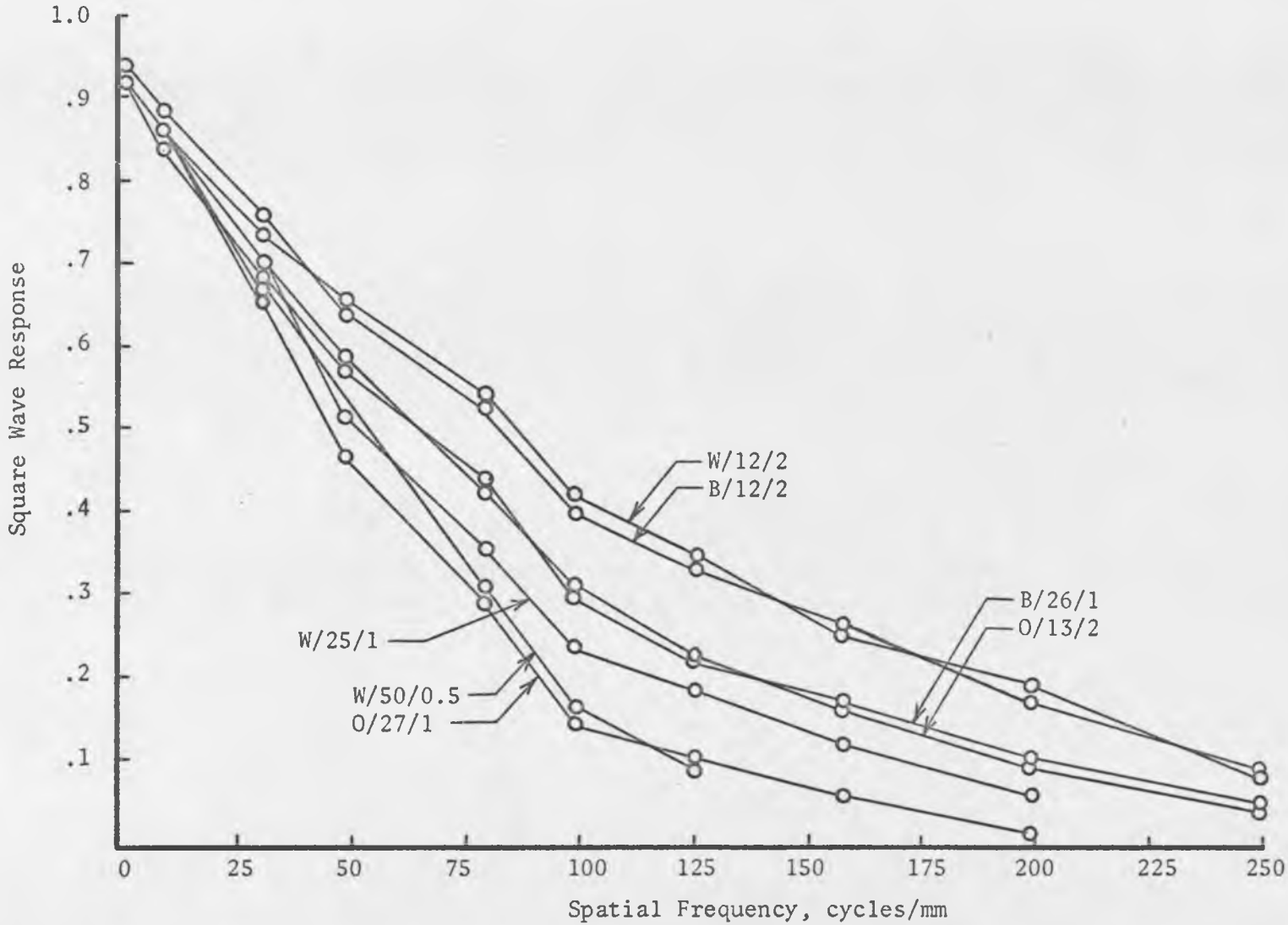

Fig. 41. On-Axis SqWR for a 8 mm Field

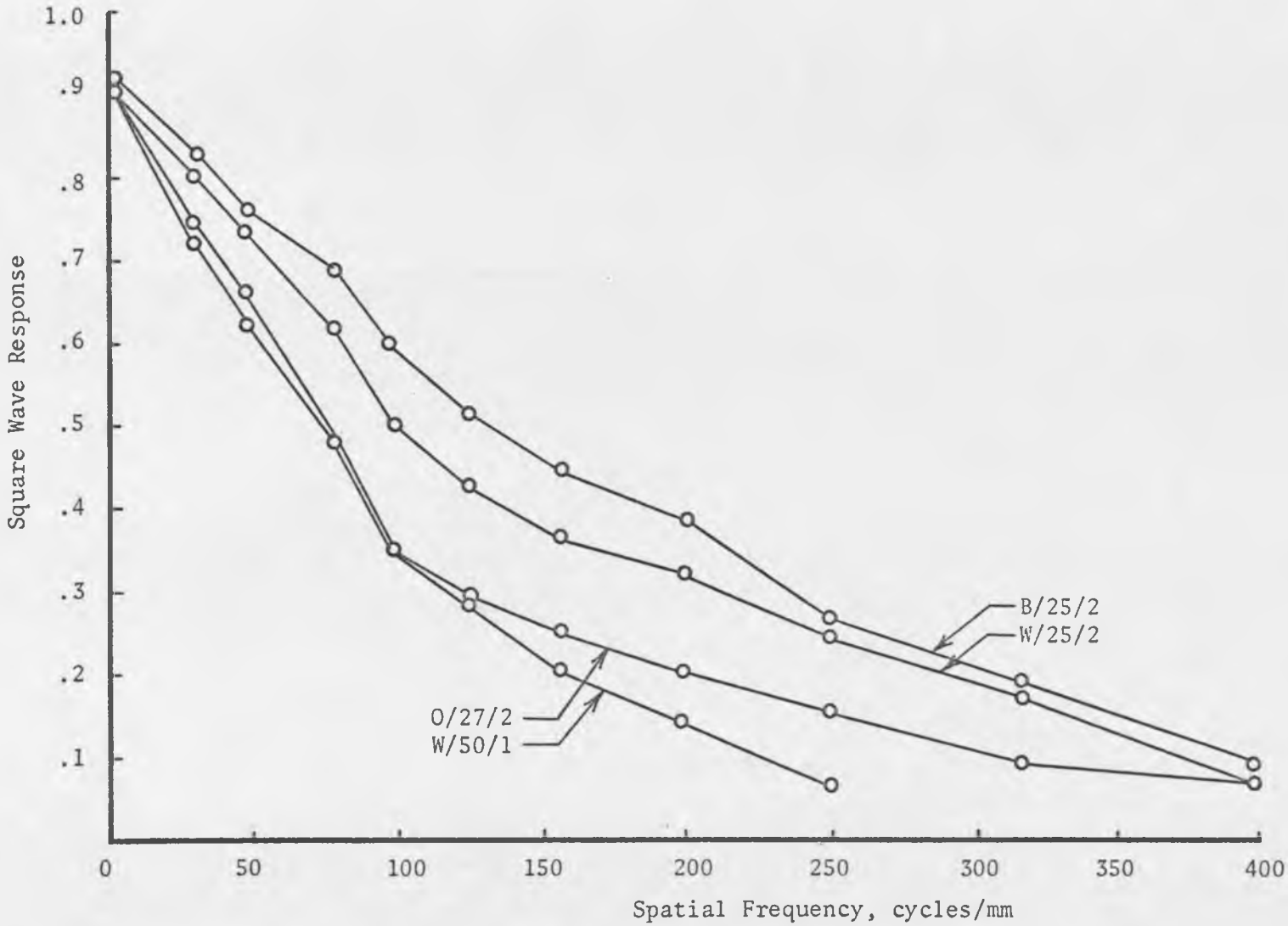

Fig. 42. On-Axis SqWR for a 4 mm Field

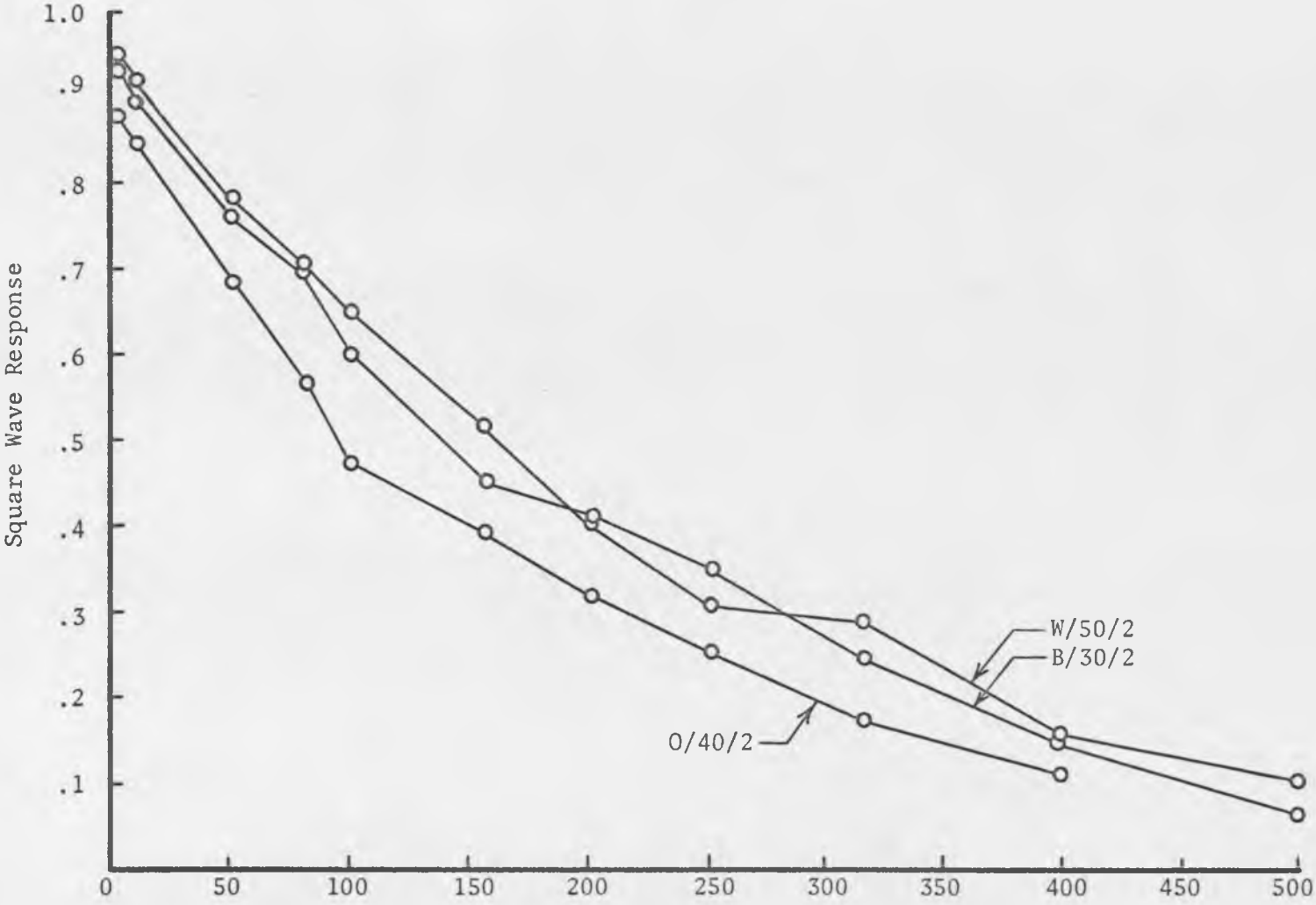

Fig. 43. On-Axis SqWR at Minimum Field Size

the 4 mm and 8 mm fields the 1 and 1a SqWR curves were averaged, but only the single orientation was used for the other curves. In Table IV the SqWR curves are ranked, one against the other. If one SqWR was not obviously better than another, then both were judged to be equal and were given the same ranking. One SqWR was judged to be better than a second if the value of the SqWR of the first was greater than that of the second over nearly the entire frequency range.

There are two generalizations which can be made from the information in Figures 39-43 and Table IV. First, the Bausch and Lomb and Wild microscopes are superior to the Olympus for on-axis viewing. The Bausch and Lomb and Wild each ranked first for 3 out of the 4 field sizes (not including the minimum field size), while the Olympus never ranked first. Second, for a given field size a microscope has a better SqWR if a high, rather than a low, power auxiliary objective is used. The two exceptions to this rule are that W/12/1 is better than W/6/2 and approximately equals W/12/0.5.

The microscope performance required for the first photointerpretation task is distinctly different from that required for the second task. When the photointerpreter is scanning or searching imagery with the microscope, he needs good performance across the entire field, not just on-axis. It is not expected that the best off-axis performance will be obtained with the microscope configuration giving the best on-axis performance. Therefore, we must compare the off-axis SqWR.

With the on-axis SqWR, the curves were directly compared and the best SqWR was easily found. However, there are seven SqWR curves

Table IV. Ranking of the Microscopes for Task 1

Field Size (mm)	Microscope	Ranking
34	B/12/0.5 W/6/1 W/12/0.5	1
	O/13/0.5	2
17	W/12/1	1
	B/12/1 W/6/1	2
	B/25/0.5 O/13/1 W/25/0.5	3
	O/27/0.5	4
8	W/12/2 B/12/2	1
	B/26/1 O/13/2	2
	W/25/1	3
	O/27/1	4
	W/50/0.5	5
4	B/25/2	1
	W/25/2	2
	O/27/2	3
	W.50/1	4
Minimum	W/50/2 B/30/2	1
	O/40/2	2

which describe the off-axis viewing for each microscope, and this is too many to be compared directly. An alternative to the direct comparison method is to characterize each curve by a meaningful number (or numbers) and then average these numbers in some way. Such a procedure is fraught with danger (Brock 1967) and can produce erroneous conclusions because a SqWR curve cannot be entirely described by a single number. However, the reduction of SqWR information in this way permits convenient comparison of numerous SqWR curves.

In order to increase the possibility of a meaningful comparison, we will describe each SqWR curve by two numbers, each describing a different characteristic of the SqWR curve. We will then compare and correlate these numbers, and thereby more validly compare the SqWR curves. The first number will be the value of the SqWR at a particular spatial frequency, which may be the cut-off frequency of the reconnaissance system that produced the imagery being viewed. One microsope is "better" than another if it has a higher response at this frequency. The frequencies used are 100 cycles/mm for the 4 mm and minimum size field, 80 cycles/mm for the 8 mm field, 50 cycles/mm for the 17 mm field, and 25 cycles/mm for the 34 mm field. For each microscope configuration there will be seven or eight of these SqWR values which are then arithmetically averaged to form a general descriptor. The descriptor characterizes the average SqWR across the field of a particular microscope configuration, but has no real physical significance itself; it is only a figure of merit. This descriptor will be called the modulation descriptor.

The second characteristic number of a SqWR curve will be the spatial frequency that corresponds to a SqWR value of 0.2. Physically, this is approximately the cut-off frequency that is observed visually if a low contrast test target (density difference of 0.20) is viewed through the microscope. Again the seven or eight numbers are simply averaged to form the frequency descriptor, a figure of merit with no real physical significance except as a tool for comparisons.

In Table V the microscopes are ranked for each field size according to the values of their modulation and frequency descriptors. Two conclusions can be made: first, the Wild microscope is ranked first for all field sizes and, therefore, is the best for task 2 type photointerpretation; and second, for a particular field size, the best performance across the field is obtained by using the lowest power auxiliary objective with the Olympus and Wild (except at the 34 mm field) microscopes, as predicted in Chapter 3. However, with the Bausch and Lomb microscope the best performance is achieved with the highest power auxiliary objective.

Many photointerpreters will have a single microscope with which to perform both the scanning (task 1) and detailed viewing (task 2) functions. In such a case we would want to know which microscope best performs both functions. By comparing Tables IV and V we find that the Wild is by far the best (the Bausch and Lomb is second, and the Olympus is third). With the Wild scanning is performed using the lowest power auxiliary objective (except at the 34 mm field) and detailed viewing is performed using the highest power auxiliary objective.

Table V. Ranking of the Microscopes for Task 2

Field Size (mm)	Microscope	Ranking	Modulation Descriptor	Frequency Descriptor
34	W/6/1	1	.16	21
	O/13/0.5		.15	21
	B/12/0.5	2	.12	18
	W.12 0.5	3	.05	12
17	W/25/0.5	1	.20	50
	B/12/1	2	.17	40
	O/27/0.5		.10	35
	O/13/1	3	.12	36
	B/25/0.5		.14	32
	W/6/2	4	.04	24
	W/12/1	5	.03	19
8	W/50/0.5	1	.27	87
	W/25/1	2	.21	80
	B/12/2	3	.16	77
	O/27/1	4	.15	64
	O/13/2	5	.13	58
	B/26/1	6	.10	45
	W/12/2	7	.03	23
4	W/50/1	1	.37	187
	O/27/2	2	.22	118
	B/25/2	3	.18	90
	W/25/2	4	.13	88
Minimum	W/50/2	1	.40	165
	O/40/2		.36	171
	B/30/2	2	.20	108

If the photointerpreter does not want to or is not able to change between various auxiliary objectives, then we may ask what microscope/lens combination best performs both tasks. Using Table V and Figures 38-42 we find that for the 34 mm field, W/6/1 is best, but B/12/0.5 is nearly as good; for the 17 mm field, B/12/1 is best; for the 8 mm field, B/12/2 is best; and for the 4 mm field, B/25/2 and 0/27/2 are about equal. Therefore, in this case the Bausch and Lomb is best.

We have used the measured SqWR curves to compare how the microscopes would perform two typical photointerpretation tasks. There are, of course, other tasks for which the microscopes can be compared and other criteria that can be used to describe the tasks which we considered. For example, a modulation of 0.3 rather than 0.2 might have been used to obtain the frequency descriptor for task 2; or the equivalent bandwidth (Shack 1956) might have been used to characterize the SqWR. When the task or criteria is changed we should not expect a particular microscope necessarily to remain the "best".

However, regardless of the manner in which the SqWR curves are evaluated, we should remember that optical performance, as reflected by the SqWR, does not completely describe how well a microscope can perform a particular task. Other considerations such as reliability, size and weight, zoom range, availability, cost, eye relief, etc. must also be weighed and evaluated in terms of the task to be accomplished. The value of the SqWR is significant, but not supreme.

LIST OF REFERENCES

Anseley, David A. and Cykowski, C. M., Collimated Light Source Study (Rome Air Development Center, Griffiss AFB, N. Y., RADC-TR-68-62, 1968), pp. 44-75

Barakat, Richard and Lerman, Steven, Diffraction Images of Truncated, One-Dimensional Periodic Target (Itek Corporation, Lexington, Mass., ATR-66-15, 1966), 25 pp.

Barnard, J. E. and Welch, F. V., Practical Photomicrography (Edward Arnold & Co., London, 1936), 210 pp.

Benford, James, The Theory of the Microscope (Bausch & Lomb, Inc., Rochester, N. Y., 1965), 33 pp.

Brock, G. C., Reflections on Thirty Years of Image Evaluation (Itek Corporation, Lexington, Mass., 1967), 16 pp.

Carpender, Vance, "The Abbe Development of Diffraction Limited MTF," Seminar Proceedings of the Society of Photo-Instrumentation Engineers, 31-34 (1969).

Coltman, John W., "Specification of Imaging Properties by Response to a Sine Wave Input," J. Opt. Soc. Am. 44, 468-471 (1954).

Department of Defense, Optical Design, MIL-HDBK-141 (U. S. Government Printing Office, Washington, D. C., 1962), pp. 26.1-26.23.

Goodman, J. W., Introduction to Fourier Optics (McGraw-Hill Book Co., San Francisco, 1968), 286 pp.

Hopkins, H. H., "Applications of Coherence Theory in Microscopy and Interferometry," J. Opt. Soc. Am. 47, 508-526 (1957).

Kohler, H. and Metzmacher, K., "The White Light Modulation Transfer Function of Optical Systems as a Function of the State of Color Correction," MTF Seminar Proceedings of the Society of Photo-Instrumentation Engineers, 195-203 (1969).

Scott, F., Scott, R. M., and Shack, R. V., "The Use of Edge Gradients in Determining Modulation Transfer Functions," Photographic Science & Engineering 7, 345-349 (1963).

Shack, R. V., "Characteristics of an Imaging Forming System," J. Res. Natl. Bur. Std. 56, 245-260 (1956).